POLITECNICO
MILANO 1863

SCUOLA DI INGEGNERIA INDUSTRIALE
E DELL'INFORMAZIONE

Techno-economic analysis of green ammonia production in innovative Catalytic Membrane Reactor

Tesi di Laurea Magistrale in
Energy Engineering - Ingegneria Energetica

Lorenzo Parisi, 991371

Advisor:
Prof. Giampaolo Manzolini

Co-advisors:
Prof. Fausto Gallucci
Dr. Iolanda Gargiulo

Academic year:
2023-2024

Abstract: Ammonia will play a crucial role in the coming years to help Europe achieve its energy goals. It can be used as a hydrogen carrier due to its superior properties compared to hydrogen: it can be liquefied at much more manageable temperatures and pressures, has a better volumetric energy density, and is not flammable. These advantages could address the storage and transportation issues associated with hydrogen.

This study involves a techno-economic analysis of a plant that employs a membrane catalytic reactor for ammonia synthesis, compared to a plant that uses conventional reactors. The study's target output is 100 tons of ammonia per day. The membrane reactor proves to be much more efficient than the series of conventional reactors, as it achieves the target with higher conversion rates and smaller volumes and quantities of catalysts. This is in contrast to the series of three conventional reactors, which require cooling to increase conversion and overcome the reaction's thermodynamic limits.

The techno-economic analysis demonstrates that the plant using the membrane reactor is slightly better than the conventional one. The membrane reactor allows for fewer components within the plant. The main cost is associated with the input feed, which remains the same in both cases due to the Haber-Bosch process's recycling of unconverted reagents.

Key-words: Ammonia synthesis, Aspen Plus, Catalytic Membrane Reactor, Haber-Bosch, Hydrogen, MATLAB, Techno-economic analysis

1. Introduction

Hydrogen is expected to play a key role in achieving EU objectives to reduce greenhouse gas emissions by a minimum of 55% by 2030 and reach net zero emissions by 2050. However, due to its low volumetric density, hydrogen is associated with storage and transportation problems. Ammonia appears to be a potential solution to the challenges with hydrogen. This study aligns with this vision as it aims to leverage the already robust infrastructure of ammonia for hydrogen transportation. The concept involves converting hydrogen into ammonia, transporting it in this form to various points of demand, and then re-converting ammonia back into hydrogen. The focus of this thesis lies in the upstream process, namely, the synthesis of ammonia. Ammonia stands as the second most produced chemical globally, with the conventional synthesis process (the Haber-Bosch process) in use for more than a century, accounting for about 1.2% of global CO2 emissions. Using renewable energy for the Haber-Bosch process holds promise in significantly reducing carbon emissions associated with ammonia production. Traditionally, this process relies on fossil fuels as the primary energy source, existing plants have been tailored to utilize natural gas (50%), oil (31%), or coal (19%) for ammonia synthesis. Replacing methane reforming with electrolysis to produce hydrogen could bring the ammonia synthesis process near the carbon neutral. The primary objective of this technical-economic analysis will be to examine the improvements that the catalytic membrane reactor can offer compared to conventional reactors. In the literature, numerous studies have conducted techno-economic analyses of ammonia production, yet none have explored the use of a membrane reactor as an alternative to the conventional reactor. Nosherwani et al. compares three methods of ammonia production that differ only in the upstream production of hydrogen and nitrogen, with the synthesis loop being the same for all three. The conventional method using steam reforming results in the lowest cost of produced ammonia at 797 $\frac{\$}{ton}$. In contrast, the methods utilizing an alkaline electrolyzer and a PEM electrolyzer, both powered by wind turbines, for hydrogen production result in costs of 917$\frac{\$}{ton}$ and 1317$\frac{\$}{ton}$, respectively [1]. Nayak-Luke et al. reported an LCOA around 1200 $\frac{\$}{ton}$ [2]. The main focus of this study is on the ammonia synthesis loop, assuming that hydrogen and nitrogen are produced using a PEM electrolyzer and a PSA (Pressure Swing Adsorption). The significant advantage of the catalytic membrane reactor lies in its ability to separate ammonia during the synthesis process, overcoming thermodynamic limits and kinetic inhibitions as the equilibrium consistently shifts towards the forward direction. This is achievable by employing highly selective membranes that possess both high permeability and mechanical as well as chemical stability. The primary transport mechanism exploited by these membranes is molecular sieving, capitalizing on the kinetic diameter differences of the three involved elements (N_2, H_2, and NH_3), with ammonia having the smallest one.

1.1. Ammonia as energy carrier

Ammonia (NH_3) contains 17.8% hydrogen (H_2) by weight, with roughly 70% of it is used in agricultural fertilizer synthesis, while the remaining 30% serves various industrial chemical purpose, including the production of plastics and explosives. Currently, the use of ammonia as an energy carrier is limited, and the majority of that is produced through fossil fuels.

Ammonia can be liquefied by either cooling it below -33°C (at atmospheric pressure) or pressurizing it above 7.5 bar (at 20°C) conditions significantly more attainable than those required for hydrogen liquefaction, which demands cooling below -253°C. The energy cost of liquefying hydrogen amounts to approximately 44.7% of its gas-phase energy. Furthermore, liquefied ammonia has an energy density of 12.92/14.4 MJ/L, compared to 8.49 MJ/L for liquid hydrogen (see Table 1.1) [3], indicating that liquefied ammonia maintains a higher volumetric energy density under less rigorous storage conditions. Moreover, ammonia exhibits a lower boil-off rate (0.025 vol%/day), enhancing its capacity to retain energy potential during extended storage and transportation over long distances. However, it is important to note that ammonia storage necessitates an additional process to extract the hydrogen before use, resulting in a slight yet noteworthy reduction in the net energy yield for every ton of hydrogen produced.

Developing a method to store renewable hydrogen within ammonia could address many of the challenges associated with hydrogen storage. The Haber-Bosch process, combining hydrogen gas with nitrogen gas to produce ammonia, offers a means to store hydrogen within ammonia. Subsequently, hydrogen can be extracted as needed by heating ammonia to high temperatures. [4]

Table 1: Characteristics comparison of H_2 and NH_3 [3];^{a}At 20°C and 10 bar ^{b}At -33°C

Properties	Units	H_2	NH_3
phase	[-]	liquid	liquid
density	[kg/m^3]	70.8	$610^a/680^b$
boiling point	[°C]	-253	-33
volumetric H_2 content	[Kg_{H_2}/m^3]	70.8	107.7/120
volumetric energy density	[MJ/L]	8.49	12.92/14.4
H_2 release	[-]	evaporation	cracking ($>$ 425 °C)
flammability/toxicity	[-]	highly flammable	toxic

Due to its extensive use as a raw material for inorganic fertilizers, there is a high level of development in many aspects of ammonia storage and transportation infrastructure. A well-established global ammonia infrastructure already exists, with considerable maritime trading of ammonia. International shipping routes are firmly established, and there is a comprehensive network of ports worldwide equipped to handle large-scale ammonia transport (see Figure 1). Leveraging this existing harbours and shipping infrastructure could facilitate the rapid adoption of large-scale ammonia transportation as an energy carrier and fuel. [5]

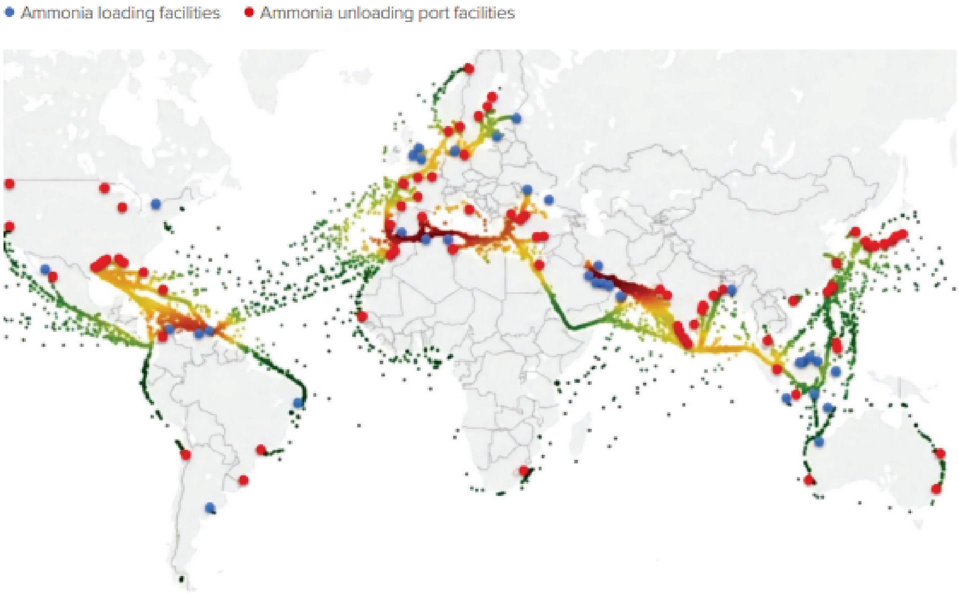
● Ammonia loading facilities
● Ammonia unloading port facilities

Figure 1: Ammonia shipping infrastructure [5]

1.2. Ammonia synthesis

The synthesis equation of ammonia is shown in (1.1)

$$H_2 + N_2 \rightarrow NH_3 \quad \Delta H_r = -92.44 \left[\frac{\text{kJ}}{\text{mol}}\right] \tag{1.1}$$

It is an exothermic reaction, according to the Le Chatelier's Principle, if the temperature is increased, the system will shift in the direction that absorbs heat to counteract the increase in temperature. Since the forward reaction is exothermic (it releases heat), the equilibrium will shift to the left, favoring the formation of reactants. If the temperature is decreased, the system will shift in the direction that generates heat, favoring the formation of NH_3.
Similarly, changes in pressure can also affect the equilibrium of the ammonia synthesis reaction. According to Le Chatelier's Principle, increasing the pressure will shift the equilibrium towards the side with fewer moles of gas. In the end, increasing the pressure will favor the formation of more ammonia.

The Haber-Bosch process, developed a century ago, accounts for 96% of ammonia production. It operates at pressures ranging from 100 to 300 bar and relies on elevated temperatures, even if this is in contrast with the thermodynamic, typically in the range of 300-500°C.
These conditions, along with specific catalysts, are employed to overcome the activation energy required to break the nitrogen triple bond and accelerate the reaction kinetics. Nitrogen dissociation represents the rate-determining step in the process.
Iron-based catalysts have historically been the primary choice for ammonia synthesis, although ruthenium has gained attention recently for its superior performance. However, its widespread use is hindered by high cost and susceptibility to hydrogen poisoning, which limits ammonia production. In contrast, iron catalysts offer a more economical and durable option.

Ammonia production plants can be divided into two sections: the first involves hydrogen production, while the second relates to the ammonia synthesis loop. In the conventional process, hydrogen is produced through steam reforming. The first reactor is fueled by external combustion, while the second is an autothermal reactor. Subsequently, the flow is sent to a reactor where the Water Gas Shift reaction occurs to minimize the CO concentration, followed by CO2 removal. The final mixture consists of hydrogen, nitrogen, methane, and argon as inert gases in the synthesis loop. The heat generated in this section of the plant is used by the steam system, compressors of the ammonia synthesis loop, and the air compressor of the secondary reformer. This typical layout is described in Figure 2.

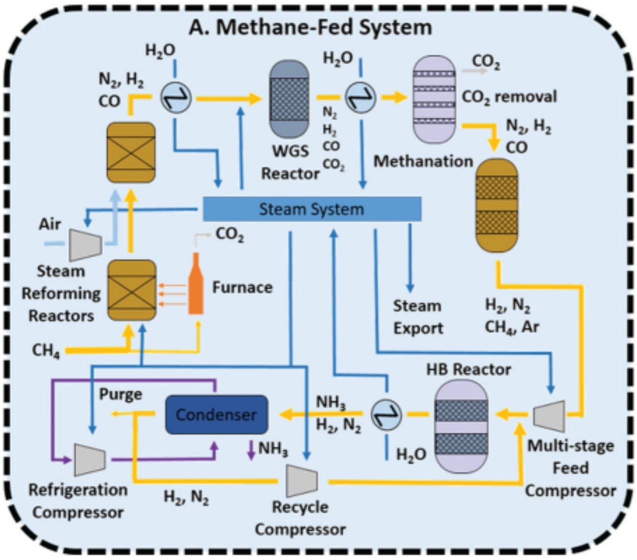
A. Methane-Fed System
H_2O
N_2, H_2
CO
H_2O
CO_2
CO_2 removal
N_2
H_2
CO
CO_2
WGS
Reactor
Methanation
N_2, H_2
CO
Air
Steam System
CO_2
Steam
Reforming
Reactors
Furnace
Steam
Export
H_2, N_2
CH_4, Ar
CH_4
HB Reactor
Purge
Condenser
NH_3
H_2, N_2
NH_3
H_2O
Multi-stage
Feed
Compressor
Refrigeration
Compressor
H_2, N_2
Recycle
Compressor

Figure 2: Methane-Fed System [6]

To enhance sustainability, the aim is to employ electrolyzers for hydrogen production and Pressure Swing Adsorption (PSA) for nitrogen production, thus reducing CO2 emissions linked to this energy-intensive process. This approach seeks to optimize the utilization of electricity generated by renewable plants. This different type of plant is shown in Figure 3.

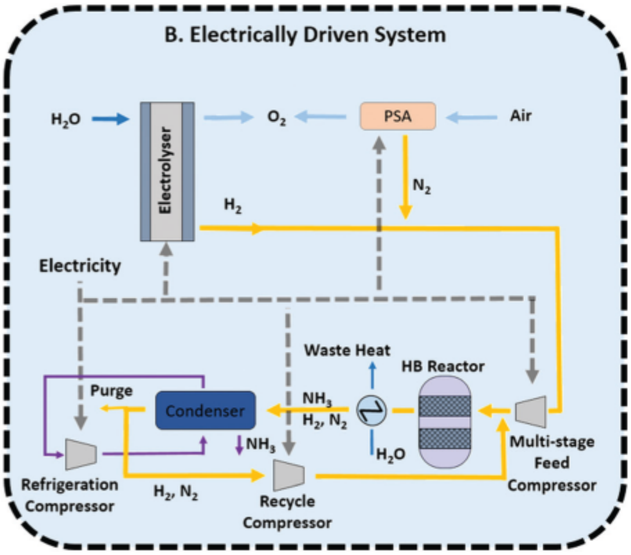
B. Electrically Driven System
H_2O
Electrolyser
O_2
PSA
Air
N_2
H_2
Electricity
Waste Heat
HB Reactor
Purge
Condenser
NH_3
H_2, N_2
NH_3
H_2O
Multi-stage
Feed
Compressor
Refrigeration
Compressor
H_2, N_2
Recycle
Compressor

Figure 3: Electrically Driven System [6]

The ammonia synthesis loop consists of a compression unit, reactors for ammonia synthesis, an ammonia separation system, a recirculation loop, and a storage unit.

The inlet stream must be adequately heated to maintain a high reaction rate, otherwise there will be low outlet temperatures that could stop the reaction. To achieve high conversion, the reactor system consists of three catalytic beds to ensure an adequate concentration of ammonia at the outlet of the final bed. The fluid exiting each reactor is cooled by quenching to shift away from equilibrium and enhance conversion in the subsequent reactor. Ammonia is separated via condensation, while unreacted nitrogen and hydrogen are recirculated after compression, and the increase in inert gases is purged and sent to the SMR furnace.

1.3. Catalytic Membrane Reactor

In this study, the conventional reactor series will be replaced by the catalytic membrane reactor, and the differences will be highlighted both technically and economically to understand the advantages and disadvantages.

A catalytic membrane reactor (CMR) is a combination of a heterogeneous catalyst and a perm-selective membrane, which is a thin film layer that allows one component of a mixture to selectively permeate through it. Membrane processes are characterized by the fact that the feed stream is divided into 2 streams: retentate and permeate. The retentate is that part of the feed that does not pass through the membrane, while the permeate is that part of the feed that does pass through the membrane. The optional "sweep" is a gas that is used to help remove the permeate [7] .

If one product preferentially permeate through the membrane, the reaction that is limited by the thermodynamic equilibrium can obtain higher overall conversion (than could be obtained in a conventional catalytic reactor), or operate at lower temperature to obtain the same conversion [8] .

The CMR operates in the following manner: the retentate, housing the catalyst, in pellet form, to facilitate ammonia synthesis, is delineated from the permeate by a carbon membrane, fortified by ceramic support to endure the elevated temperatures inherent to the process. The ammonia synthesis reaction occurs only in the retentate and the NH_3 produced diffuse through the membrane. Simultaneously, external to the retentate, the sweep gas, flowing congruently with the feed, aids in permeate extraction while enhancing heat transfer between retentate and permeate. (See Figure 4)

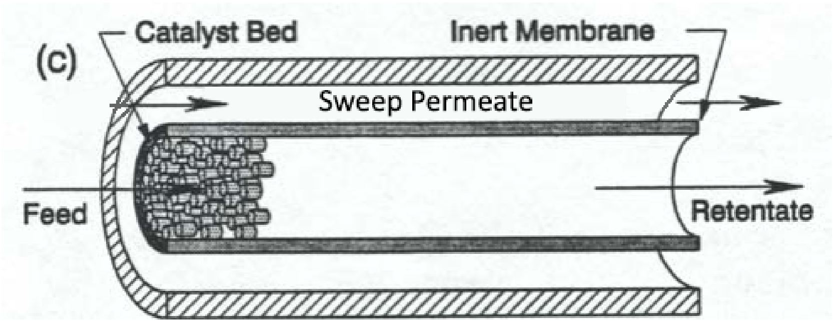

Figure 4: Architecture of the Catalytic Membrane Reactor

The main mechanism of gas transport through membranes are: Knudsen diffusion, viscous flow, selective adsorption and surface diffusion and molecular sieving. The latter will be the one exploited by the carbon membrane adopted in this study.

1.4. Catalysts

As stated before the ammonia synthesis reaction is influenced by low temperatures and high pressures. Nevertheless, equilibrium conditions constitute a fraction of the overall picture, as thermodynamics fails to offer insight into reaction rate.

The reaction mechanism for the catalyzed reaction of nitrogen and hydrogen to form ammonia are as follow:

$$N_2 +^* \rightleftharpoons N_2^* \tag{1}$$

$$N_2^* +^* \rightleftharpoons 2N^* \tag{2}$$

$$H^* + N^* \rightleftharpoons NH^* +^* \tag{3}$$

$$NH^* + H^* \rightleftharpoons NH_2^* +^* \tag{4}$$

$$NH_2^* + H^* \rightleftharpoons NH_3^* +^* \tag{5}$$

$$NH_3^* \rightleftharpoons NH3 +^* \tag{6}$$

$$H_2 + 2^* \rightleftharpoons 2H_2^* \tag{7}$$

The chemisorption of nitrogen (Eq. 2) is the rate-limiting step. [9]

The chemisorption include the dissociative adsorption which refers to the breaking of molecular bonds as the adsorbate molecules adhere to the surface of the adsorbent. N_2 molecules are adsorbed onto the catalyst surface, and the strong triple bond of N_2 is broken during this process. This dissociation of the nitrogen molecule allows the nitrogen atoms to bind to the surface of the catalyst, where they can subsequently react with hydrogen atoms to form ammonia molecules. Due to the considerably energy demand for nitrogen dissociation, the reaction does not proceed at ambient temperatures. Nitrogen dissociation typically occurs in gas phase around 3000°C, while hydrogen dissociates significantly only at temperatures exceeding 1000°C. Consequently, executing the reaction at lower temperatures is impractical due to the energy requirement and by raising the temperature the reverse reaction predominates. This dilemma underscores the significance of the iron catalyst adopted. Energy profiles for ammonia synthesis, illustrated in Figure 1.6, indicate a substantial reduction in activation energy when the catalyst is present. The hydrogen and nitrogen molecules loose their translational degrees of freedom when bound to the catalyst surface and the forward reaction occurs. The necessity of extremely high temperature is obviated but temperatures between 250°C-500°C are still required to dissociate N_2 and H_2 molecules, even with a catalyst. [10]

1.5. Membranes

Gas transport through porous media is influenced by various factors, including pore size and distribution across the membrane layer, the interaction between gas molecules and pores, and the void-free volume. It is widely acknowledged that there are four distinct transport mechanisms: Knudsen diffusion, viscous flow, selective adsorption and surface diffusion and molecular sieving. [11]

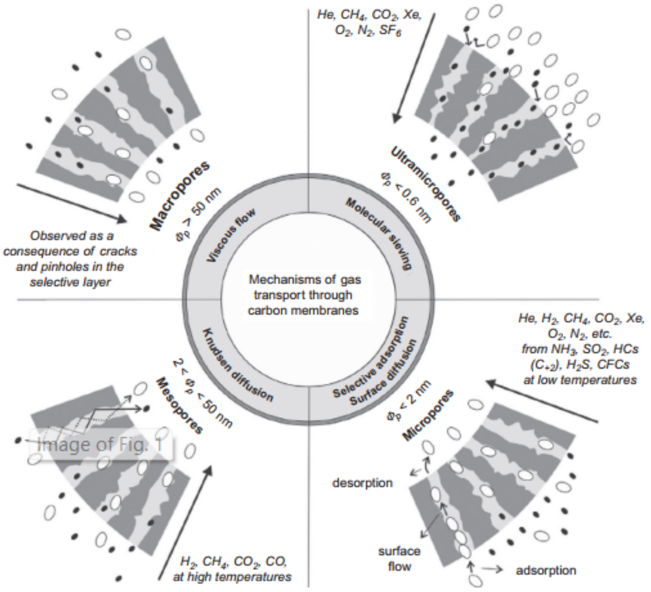
He, CH₄, CO₂, Xe, O₂, N₂, SF₆
Ultramicropores
ϕp < 0.6 nm
Molecular sieving
Macropores
ϕp > 50 nm
Viscous flow
Observed as a consequence of cracks and pinholes in the selective layer
Mechanisms of gas transport through carbon membranes
He, H₂, CH₄, CO₂, Xe, O₂, N₂, etc. from NH₃, SO₂, HCs (C₊₂), H₂S, CFCs at low temperatures
Selective adsorption
Surface diffusion
ϕp < 2 nm
Micropores
desorption
surface flow
adsorption
Knudsen diffusion
2 < ϕp < 50 nm
Mesopores
H₂, CH₄, CO₂, CO, at high temperatures

Figure 5: Transport Mechanism through Carbon membranes

Polymer membranes play a crucial role in separating permeative gases. While organic polymer membranes may lack durability in high temperatures and harsh environments, they can undergo transformation through pyrolysis into carbon. As an inorganic material, carbon membranes exhibit superior thermal and chemical stability compared to their polymer counterparts. Additionally, serving as molecular sieve pore membranes, they offer heightened selectivity over conventional polymeric membranes, which operate based on a solubility-diffusivity principle [12].

Molecular sieving emerges as the predominant transport mechanism in carbon membranes for selectively separating certain gas pairs, where gases are separated based on their kinetic diameters. This mechanism predominantly operates in ultramicropores ($d_p < 0.60\ nm$). The pores exhibit a similar order of magnitude as the kinetic diameter of the gases, effectively acting as filters that permit the passage of certain gases while impeding larger ones. The molecular sieve transport mechanism is particularly noteworthy for the separation of gas pairs with noticeable disparities in kinetic diameter.

Table 2 illustrates the different kinetic diameters of the species participating in the ammonia synthesis reaction, with ammonia exhibiting the smallest one. [13]

Table 2: Kinetic diameter of NH_3, H_2 and N_2

Property	NH_3	H_2	N_2
Kinetic Diameter	0.260 nm	0.289 nm	0.364 nm

The flux of a gas through the different pores can be described according to Fick's first law as stated in Eq. 8:

$$J_i = -D_i \cdot \frac{\partial C}{\partial x} \tag{8}$$

where J_i is the gas flux $\left[\frac{mol}{m^2 \cdot s}\right]$ through the membrane, which is a function of the diffusivity of the gas D_i and the gradient of gas concentration C through the pore length x. The gas diffusion coefficient for the molecular sieving mechanism can be expressed as stated in Eq. 9:

$$D_i = D_i^0 \cdot exp\left(\frac{-E_{act}}{R \cdot T}\right) \tag{9}$$

Assuming the ideal gas law, the gas flux associated with the molecular sieving contribution can be written as Eq 10, with E_{ads} as the energy of adsorption $\left[\frac{kJ}{mol}\right]$:

$$J_i = \frac{\Delta p}{RTL} \cdot D^0\left(T\right) \cdot exp\left[\frac{-\left(E_{act,i} - E_{ads}\right)}{RT}\right] \tag{10}$$

In the case of molecular sieving, the E_{act} for the transport through constrictions related to ultramicropores will always be higher that the adsoprtion energy, and thus the gas permeation will always be increased with an increase in the temperature $(E_{act} - E_{ads} > 0)$ [11] .

2. Method

The analysis is divided into two levels: the first concerns the reactor model, while the second pertains to the plant analysis, which was performed using Aspen Plus, followed by the economic analysis.

The reactor model has been developed using MATLAB. This model is 1D to simplify the reactor geometry and the chemical processes within it. The dimension where reactants and products flow is the axial one. Subsequently, the MATLAB model is called by Aspen to simulate the entire process, a process simulation software used in the chemical and associated industries for modeling, designing, and optimizing chemical processes, to simulate the entire process.

In this chapter, all equations, parameters governing the reaction kinetics, mass and heat exchange between retentate and permeate, and the various components adopted within the loop of ammonia synthesis will be described.

2.1. Kinetics

The kinetic adopted for a comercially available ammonia synthesis Fe catalyst is represented in Eq. 11 [14]:

$$r_{\mathrm{N2}} = 2k\left[K_{\mathrm{eq}}^2 \cdot a_{\mathrm{N2}}\left(\frac{a_{\mathrm{H2}}^3}{a_{\mathrm{NH3}}^2}\right)^{\alpha} - \left(\frac{a_{\mathrm{NH3}}^2}{a_{\mathrm{H2}}^3}\right)^{1-\alpha}\right] \tag{11}$$

The kinetic adopted for the Ruthenium catalyst is represented in Eq. 12 [15] :

$$r_{\mathrm{N2}} = k \cdot \lambda \cdot \frac{a_{N_2}^{0.5}\left[\frac{a_{H_2}^{0.375}}{a_{NH_3}^{0.25}}\right] - \frac{1}{K_{eq}}\left[\frac{a_{NH_3}^{0.75}}{a_{H_2}^{1.125}}\right]}{1 + K_{H_2}a_{H_2}^{0.3} + K_{NH_3}a_{NH_3}^{0.2}} \tag{12}$$

k is the kinetic constant for the reverse reaction, K_{eq} is the equilibrium constant of the reaction, a_i are the activities of the components, and α is a constant parameter.

Some thermodynamic data are required to relate activities a_i to the composition, temperature and pressure. For this purpose it has been used:

The Lewis and Randall rule (1961): this is known to be valid in the temperature and pressure range that has been considered.

The activity of a gas is given by definition as:

$$a_i = \frac{f_i}{f_i^*} \tag{13}$$

where f_i is the fugacity of the component i, and f_i^* is the fugacity of the pure component at a pressure of 1 atm at the temperature of the system.
The activity a_i can be written as:

$$a_i = f_i = \phi_i \cdot y_i \cdot P \tag{14}$$

where ϕ_i is the fugacity coefficient of component i, y_i is the molar fraction of the component i, P is the pressure in atm.

For the Hydrogen's activity coefficient it has been used the correlation from Cooper (1967) and Shaw and Wones (1964):

$$\begin{aligned}\phi_{\mathrm{H}_2} = \exp\Bigg\{ &\exp\bigg(-3.84021 \cdot 0.125 \cdot T + 0.541\bigg) \cdot P - \exp\bigg(-0.1263 \cdot T^{0.5} - 15.980\bigg) \cdot P^2 \\ &+ 300\bigg[\exp\bigg(-0.011901 \cdot T - 5.941\bigg)\bigg]\bigg(\exp\bigg(-\frac{P}{300}\bigg) - 1\bigg)\Bigg\}\end{aligned} \tag{15}$$

For nitrogen and ammonia, the correlations of Cooper (1967) and Newton (1935) have been modeled by the following expressions:

$$\phi_{\mathrm{N}_2} = 0.93431737 + 0.3101804 \cdot 10^{-3} \cdot T + 0.295896 \cdot 10^{-3} \cdot P - 0.2707279 \cdot 10^{-6} \cdot T^{-2} + 0.4775207 \cdot 10^{-6} \cdot P^2 \tag{16}$$

$$\phi_{\mathrm{NH}_3} = 0.1438996 + 0.2028538 \cdot 10^{-2} \cdot T - 0.4487672 \cdot 10^{-3} \cdot P - 0.1142945 \cdot 10^{-5} \cdot T^2 + 0.2761216 \cdot 10^{-6} \cdot P^2 \tag{17}$$

To calculate the equilibrium constant it has been used the equation of Gillespie and Bettie (1930):

$$\log_{10}(K_{eq}) = -2.691122 \cdot \log_{10} T - 5.519265 \cdot 10^{-5} T + 1.848863 \cdot 10^{-7} + T^2 + \frac{2001.6}{T} + 2.6899 \tag{18}$$

The equation of reverse ammonia synthesis reaction has been considered in base of Arrhenius format:

$$k = k_0 \cdot \exp\left(\frac{-E}{R \cdot T}\right) \tag{19}$$

Where :
- $k_{Fe} = 8.849 \cdot 10^{14}$ pre-exponential factor
- $E_{Fe} = 40765$ Activation energy
- $k_{Ru} = 9.02 \cdot 10^{8}$ pre-exponential factor
- $E_{Ru} = 23000$ Activation energy
- $R = 1.987\left[\frac{cal}{mol \cdot K}\right]$ Universal gas constant
- T is the Temperature in degrees Kelvin

The two kinetics were validated according to these two studies: the one concerning the iron catalyst was validated based on Nielsen's work [16], while the one concerning the ruthenium catalyst was validated based on Rossetti's research [15].

2.2. Reactor Model

In this section, all the parameters and properties that characterize the Matlab model simulating the reaction within the membrane reactor and also the conventional reactor will be introduced.

The assumption regarding the reactor model simulated on Matlab are:
- 1D model
- Peng-Robinson themodynamic model
- Negligible pressure drop
- Real gas behaviour
- $\frac{L}{D} = 3$

The model solves a system of ODEs and takes as inputs the molar flow rates of each component, the temperatures of the retentate and permeate, the pressures, and the input data characterizing the reactor and the membrane (see Table 3-4). For each integration step, it calculates the partial pressures of each component and the reaction rate according to Eq. 11 and 12. It also determines the flux of each component through the membrane based on Eq 21, ensuring mass and energy balances described in Eq.(22-25).
The conversion χ_{N_2} was analyzed at various values of gas hourly space velocity (GHSV) defined as in Eq.7 because the reaction occurs only in the retentate.

$$GHSV = \frac{\frac{F_{in_{ret}}}{\rho_{NC}}}{V_{tot} \cdot (1-\epsilon)} \quad \left[\frac{1}{h}\right] \tag{20}$$

In Table 2 are shown the parameters chosen to characterize a catalytic reactor, which include: the diameter of the catalyst particle d_p, the catalyst particle density ρ_c, the catalyst dilution factor D_{cat} and the bed voidage ϵ.

Table 3: Catalyst bed parameters

Parameter	Value	Unit
d_p	$2.5 \cdot 10^{-3}$	m
D_{cat}	$\frac{1}{3}$	$[-]$
$\rho_{c_{Fe}}$	2800	$\frac{kg}{m^3}$
$\rho_{c_{Ru}}$	590	$\frac{kg}{m^3}$
ϵ	0.4	$[-]$

Table 3 presents key data used to characterize the membrane: D_m^o and D_m^i are the external and the internal diameter of the membrane, σ_{NH_3/H_2} and σ_{NH_3/N_2} the ammonia selectivity concerning both hydrogen and nitrogen, $\mathcal{P}_{\mathcal{NH}_{\ni}}$ the ammonia permeability and $Sweep_{gas}$ is the required amount of sweep gas , defined in this instance as the molar inflow rate into the retentate.

Table 4: Membrane reactor parameters

Parameter	Value	Unit
D_m^o	$10 \cdot 10^{-3}$	m
D_m^i	$7 \cdot 10^{-3}$	m
$\mathcal{P}_{\mathcal{NH}_{\ni}}$	$4 \cdot 10^{-7}$	$[-]$
σ_{NH_3/H_2}	50	$[-]$
σ_{NH_3/N_2}	1000	$[-]$
$Sweep_{gas}$	$F_{in_{ret}}$	$[\frac{kmol}{hr}]$

J_i is the flux of the component i passing through the membrane, which is calculated according to Eq. (7). It is considered to be positive when the flow is going from retentate to permeate.

$$J_i = \mathcal{P}_{\rangle} \cdot \left(P_i^R - P_i^P\right) \tag{21}$$

$\mathcal{P}_{\rangle}$ $\left[\frac{mol}{Pa \cdot s \cdot m^2}\right]$ accounts for the permeance of each gas, while P_i^R and P_i^P accounts for the partial pressure of each gas of the retentate and permeate side.
The mass balance for both retentate and permeate side are presented in this section. For each component we have the following equations:

$$\frac{dF_i^R}{dL} = \theta_i \cdot r_i \cdot \rho_c \cdot (1-\epsilon) \cdot \frac{\pi}{4} \cdot \left(D_r^2 - D_m^{o^2}\right) - J_i \cdot (\pi \cdot D_m^o) \tag{22}$$

$$\frac{dF_i^p}{dL} = J_i \cdot (\pi \cdot D_m^o) \tag{23}$$

Where θ_i is the stoichiometric coefficient, r_i is the reaction rate, ρ_c is the catalyst density. D_r is the diameter of the reactor.
Likewise the mass balance, the energy balance equations are computed for the retentate and the permeate side.

$$\frac{dT^R}{dL} = \frac{r \cdot (-\Delta H_R) \cdot \rho_c \cdot (1-\epsilon) \cdot \frac{\pi}{4}\left(D_r^2 - D_m^{o^2}\right)}{\sum_i F_i^R \cdot cp_i^R} - \frac{U \cdot N_m \cdot \pi \cdot D_m^i \cdot \left(T^R - T^P\right)}{\sum_i F_i^R \cdot cp_i^R} \tag{24}$$

$$\frac{dT^P}{dL} = \frac{U \cdot N_m \cdot \pi \cdot D_m^i \cdot \left(T^R - T^P\right)}{\sum_i F_i^P \cdot cp_i^P} \tag{25}$$

Where N_m is the number of the membrane adopted inside the reactor and U is the global heat transfer coefficient, which describes three heat transfer phenomena:

1. The convection in the inner tube
2. The conduction through the membrane
3. The convection in the outer tube

$$U = \left[\frac{1}{h^P} + \frac{\frac{Dm^i}{2} \cdot 2 \cdot \ln \frac{D_r}{D_m^i}}{k} + \frac{D_m^i}{D_r} \cdot \frac{1}{h^R}\right]^{-1} \tag{26}$$

The heat transfer coefficient in the reaction zone , h^R , has been calculated according to the correlation of Li and Finalyson [17] , Eq. 33 which takes in account the heat transfer of a packed bed by referring to a Reynold's number depending on particle diameter. As for permeate zone, h^P, has been calculated according to the correlation of Dittus-Boelter described in Eq. 34 which consider a smooth concentric anulus [18]. Lastly the conductivity, which is referred in this case to a carbon membrane, has been calculated as contribution of the carbon layer thermal conductivity and $\alpha - Al_2O_3$ (the membrane support) thermal conductivity through a correlation [19].

$$Re^R = \frac{d_p G^R}{\mu_{mix}^R} \tag{27}$$

$$Re^P = \frac{(D - D_m^o) \cdot G^P}{\mu_{mix}^P} \tag{28}$$

$$G^R = \frac{F_{tot}^R Mw_{mix}^R}{A} \tag{29}$$

$$G^P = \frac{F_{tot}^P Mw_{mix}^P}{A_m^i} \tag{30}$$

$$Pr^R = \frac{\mu_{mix}^R \cdot cp_{mix}^R}{\lambda_{mix}^R} \tag{31}$$

$$Pr^P = \frac{\mu_{mix}^P \cdot cp_{mix}^P}{\lambda_{mix}^P} \tag{32}$$

$$Nu^R = 0.017 \cdot {Re^R}^{0.79} = \frac{h^R \cdot d_p}{\lambda_{mix}^R} \tag{33}$$

$$Nu^P = 0.0023 \cdot {Re^P}^{0.8} \cdot {Pr^P}^{0.4} = \frac{h^P \cdot D_m^i}{\lambda_{mix}^P} \tag{34}$$

2.3. Aspen Model

Aspen Plus was used to simulate the ammonia synthesis loop with both the conventional reactor and the membrane reactor. The two loops for synthesizing ammonia are described in this chapter. The main difference between the loop employing the membrane reactor is that it utilizes a single reactor instead of three reactors in series. The separation system is the same for both, and they both employ a recirculation to convert unreacted gases in the reaction.

The main assumption adopted in Aspen Plus are:

- Math Model → Peng-Robinson EoS
- Steady-State Model
- Target Output = 100 $\frac{ton_{NH3}}{day}$
- NH_3 purity > 99.9%
- GHSV = 1000

Table 5: Aspen assumptions

Parameter	Value	Unit
Δp	0	bar
ΔT_{app}	10	°C
η_{iso}	87	%
η_{mecc}	95	%
T_{cond}	-85	°C
U_{HX}	0.02	$\frac{kW}{m^2K}$

The conventional ammonia synthesis loop, shown in Figure 6, includes three reactors arranged in series to address thermodynamic and kinetic limitations. After each reactor, the gas is cooled to improve overall conversion. In contrast, the loop with a membrane reactor requires only a single reactor. Subsequently, the ammonia-rich gas is cooled and separated through condensation, while the unconverted reactants are recirculated.

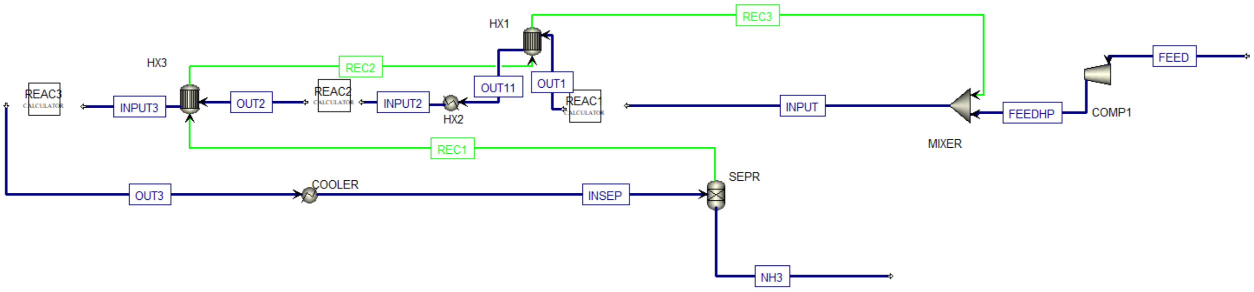
HX1
REC3
FEED
HX3
REC2
OUT11
OUT1
REAC3
CALCULATOR
INPUT3
OUT2
REAC2
CALCULATOR
INPUT2
HX2
REAC1
CALCULATOR
INPUT
FEEDHP
COMP1
MIXER
REC1
SEPR
OUT3
COOLER
INSEP
NH3

Figure 6: Layout of the plant adopting the conventional reactors

The loop of ammonia synthesis with the membrane reactor is shown in Figure 7. The difference from the conventional setup is the adoption of only one reactor and one heat exchanger. The majority of the ammonia resides in the permeate,z so the separation will only occur for this stream.

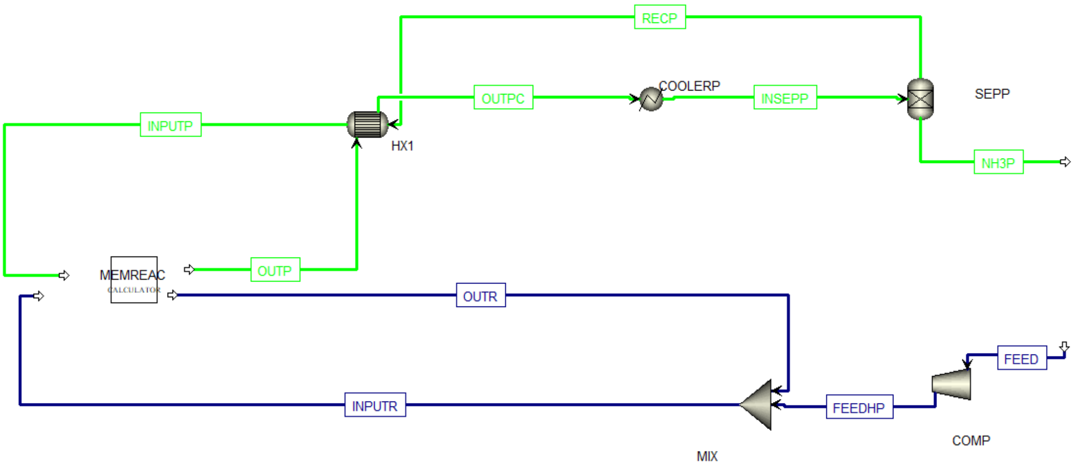
RECP
OUTPC
COOLERP
INSEPP
SEPP
INPUTP
HX1
NH3P
MEMREAC
CALCULATOR
OUTP
OUTR
FEED
INPUTR
FEEDHP
COMP
MIX

Figure 7: Layout of the plant adopting the membrane reactor

2.4. Economic Model

The economic analysis was conducted using the NETL (National Energy Technology Laboratory) [20] approach, which differentiates between the capital (CAPEX) and operational (OPEX) costs of an industrial plant. These costs are then used to determine the final production cost of the ammonia produced according to the Eq. 34:

$$COP = \frac{OPEX + CAPEX_{\text{yearly}}}{\text{ton}_{NH_3\ \text{yearly}}} \left[\frac{€}{\text{ton}_{NH_3}}\right] \tag{35}$$

The determination of the CAPEX follows the approach outlined in Table 7. Primarily, it is necessary to calculate the BEC (Bare Erected Cost), which is the sum of the cost of the equipment within the plant. In the Eq. 36 it is shown how all components cost are calculated. Q_b is a capacity in terms of the scaling parameter of the known base reference, M is a constant depending on the equipment type, f_p, f_t and f_m are indexes that account for the material of construction, the pressure and the temperature. The CEPCI (Chemical Engineering Plant Cost Index) is a tool for chemical process industry to compare plant construction from one period to another.

$$C_E = \frac{CEPCI_{2023}}{CEPCI_{\text{ref}}} \cdot \left(\frac{Q}{Q_b}\right)^M \cdot f_p \cdot f_t \cdot f_m \tag{36}$$

To calculate the cost of the membrane reactor, it has been used the Eq. 37 and the parameters listed in Table 6. [21]

$$C_{reactor} = 10^{\left(k1+k2\cdot\log(V)+K3[\log(V)]^2\right)} f_M \cdot \frac{CEPCI_{2023}}{CEPCI_{\text{ref}}} \tag{37}$$

Table 6: Parameters for the reactor cost estimation [21]

Component	K_1	K_2	K_3	FM	$CEPCI$	$CEPCI_{REF}$
Reactor	3.5	0.45	0.11	4	789.2	596.2

Once the BEC has been calculated, it is then possible to compute the TOC (Total Overnight Costs).

Table 7: Methodology for the calculation of TOC [22]

Index	Cost (M€)
Total Installation Cost (TIC)	80% BEC
Total Direct Plant Cost (TDPC)	BEC + TIC
Indirect Costs (IC)	14% TDPC
Engineering Procurement and Construction (EPC)	TDPC + IC
Contingency and Owner's Costs (C&OC)	
Contingency	10% EPC
Owner's Cost	5% EPC
Total Overnight Costs (TOC)	EPC + C&OC

The OPEX (Operating Expenditure) is calculated as follow using Eq. 38.

$$OPEX\left[\frac{M€}{y}\right] = OPEX_{feedstock} + OPEX_{utilities} + OPEX_{O\&M} + OPEX_{variables} \tag{38}$$

The $OPEX_{feedstock}$ represents the expenses sustained in supplying the hydrogen and the nitrogen, excluding the transportation cost due to the specific location of the plant. The $OPEX_{utilities}$ is the cost associated to the refrigerants, the cooling water and the electricity to supply the pumps and the compressors. The $OPEX_{O\&M}$ accounts for labor, maintenance and insurance costs and the $OPEX_{variables}$ are the cost associated with catalyst and membranes.

The operating expenses related to the various streams were calculated using Eq. 39.

$$OPEX_i\left[\frac{M€}{y}\right] = C_i \cdot \dot{m}_i \cdot h_{avail} \cdot 10^{-6} \tag{39}$$

Wehre the parameters adopted are listed below:

- C_i is the specific cost of the i variable
- $\dot{m}_i$ is the flow rate of the i variable
- h_{avail} represents the annual operating hours assumed for the plant. In this instance, a value of 7884 hours has been selected, equivalent to 90% of the total hours in a year.

The OPEX related to the membrane and the catalyst cost are described in Eq 40 and Eq 41, where A_m represent the membrane area utilized and Kg_{cat} the quantity of iron catalyst inside the reactor.

$$OPEX_{\text{membrane}} = C_{mem} \cdot Mem_{lifetime} \cdot A_m \tag{40}$$

$$OPEX_{\text{catalyst}} = C_{\text{cat}} \cdot Cat_{lifetime} \cdot Kg_{cat} \tag{41}$$

All the assumption adopted for the OPEX calculation are listed in Table 8.

Table 8: Methodology for the calculation of the OPEX

Index	Unit	Cost (M€)
H_2	$\frac{€}{kg}$	5.905 [1]
N_2	$\frac{€}{m^3}$	0.250 [2]
$Fe_{catalyst}$	$\frac{€}{kg}$	0.1607 [23]
$Membrane$	$\frac{€}{m^2}$	93 [24]
Electricity	$\frac{€}{kWh}$	0.085
Cooling Water	$\frac{€}{ton}$	0.013
Labor	$\%TOC$	1
Maintenance	$\%TOC$	2.5
Insurance	$\%TOC$	2

To assess the yearly capital expenditures, ensuring a comprehensive understanding of a long-term financial implication, the yearly capex is calculated as follow in Eq. 43. The parameters for the calculation of the Capital Cost recovery Factor are:

- i = 8%, discount rate [25]
- n = 20 years, the lifetime of the plant

$$CCF = \frac{i \cdot (1+i)^n}{(1-i)^n - 1} \tag{42}$$

$$CAPEX_{\text{yearly}} = TOC \cdot CCF \tag{43}$$

2.5. Reactor Analysis

In this section, the most significant analysis leading to the selection of the final configuration for both the conventional reactor and the membrane one will be presented.

These simulations were conducted using a constant molar inlet flow rate of 100 kmol/hr, adopting a $\frac{H_2}{N2}$ ratio equal to 3, while varying the volume. The range of inlet temperatures investigated for the feed entering the retentate spans from 370°C to 495°C, as this is the range in which the iron catalyst is active [16], while for the ruthenium catalyst the inlet temperatures spans from 320 °C to 480°C . [15].The pressure drops were neglected for simplicity.

---

[1] H2 cost, https://www.iea.org/data-and-statistics/charts/indicative-production-costs-for-hydrogen-via-electrolysis-in-selected-regions-compared-to-current-references-2

[2] Nitrogen cost (High Volume Users) https://puritygas.ca/revisiting-the-costs-of-nitrogen-gas/

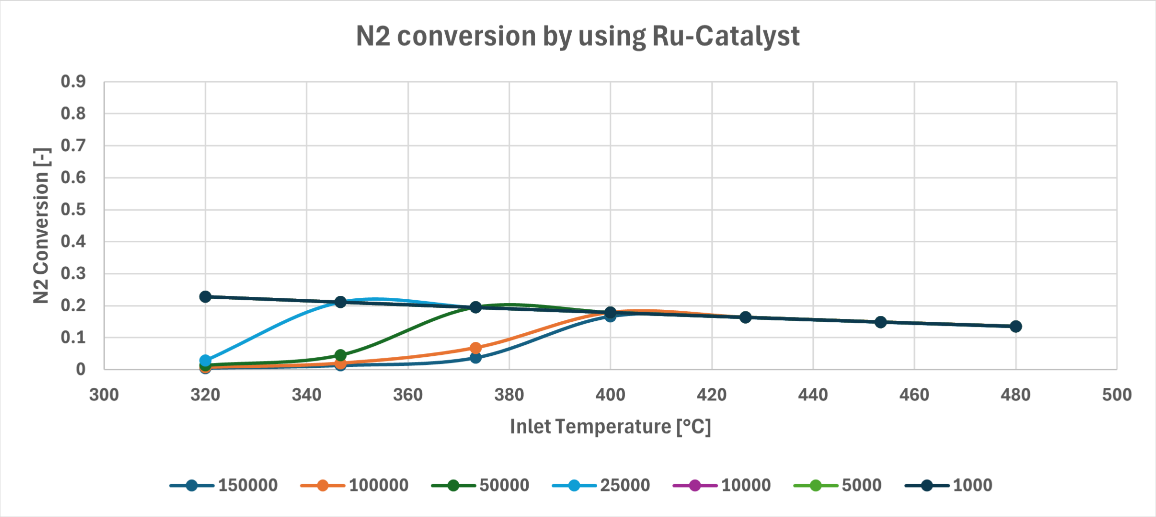

Figure 8: Conversion of the Conventional Reactor varying the inlet temperature with Ru catalyst

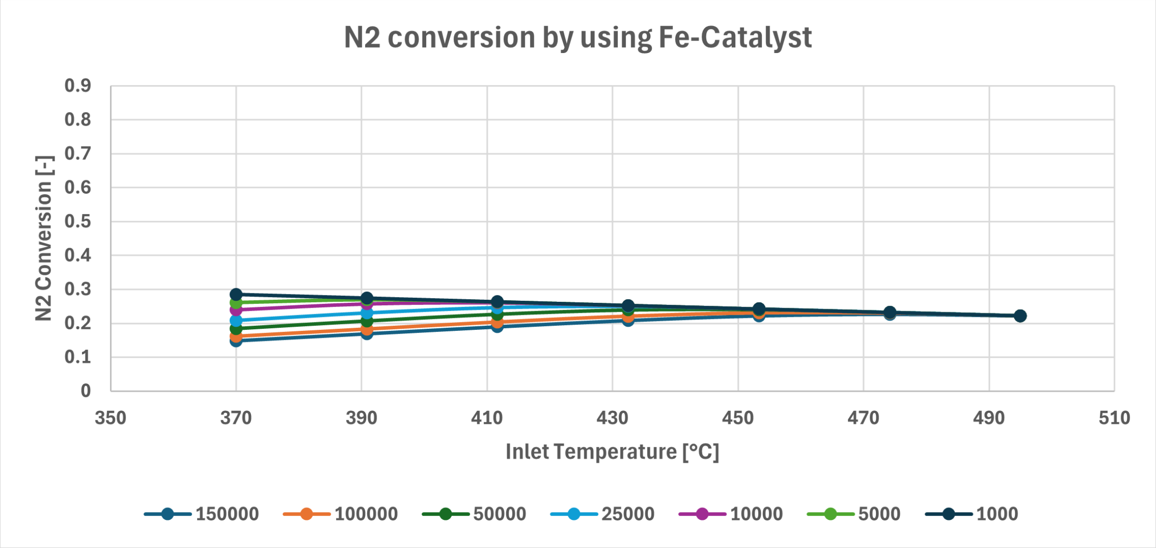

Figure 9: Conversion of the Membrane Reactor varying the inlet temperature with Fe catalyst

These two graphs shows that at low GHSV, both kinetics reach a plateau, and the one using Fe-catalyst exhibits higher conversion ($@GHSV = 1000 \rightarrow 28.49\%\ vs\ 22.82\%$). For this reason, it was decided to proceed with the iron catalyst.

For the membrane reactor a membrane area of 10 m^2 was adopted, with the retentate pressure fixed at 200 bar and the permeate pressure at 30 bar [3]. The latter was assumed because it was hypothesized that the hydrogen originates from a PEM electrolyzer operating at 30 bar.
Both Figure 7 and Figure 8 clearly demonstrate that reducing the space velocity enhances the conversion rate of the process. In the membrane reactor, decreasing the space velocity (achieved in this case by increasing the volume) results in higher conversion rates. This occurs due to a decrease in residence time and also because, with an increased volume and a fixed membrane area, the impact of the membrane intensifies. The temperature maximum associated with conversion shifts to the right.

---

[3] PEM electrolyzer, https://nelhydrogen.com/product/m-series-electrolyser/

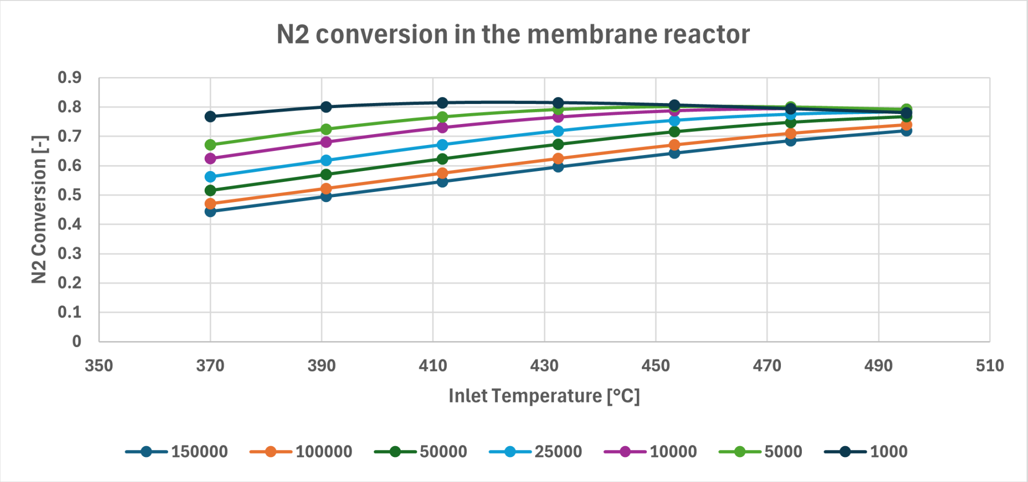

Figure 10: Conversion of the Conventional Reactor varying the inlet temperature

The set objective for this technical-economic analysis is to achieve a production of 100 tons of ammonia per day. The goal is to minimize the reactor dimensions to meet the assumed target. Subsequent section illustrate how various input parameters affect the conversion, the ammonia recovery, and outlet temperatures of both permeate and retentate.

2.5.1 Effect of the Sweep gas

The function of the sweep gas is to facilitate the extraction of the permeate and improve the heat exchange within the reactor. Since we are able to separate almost 100% of the produced ammonia in the retentate, by increasing the area of the membrane, reducing the amount of sweep gas produced can bring many benefits to the plant. Given the utilization of a porous membrane and the possibility of back permeation, the sweep gas is composed of the same reactants as the feed to prevent contamination of the retentate with additional gases. A large amount of it implies the use of heat exchangers and separators with very high surfaces to cool and separate this flow.

In Figure 11, it can be observed that reducing the amount of sweep gas, while keeping the same GHSV, inlet temperature, membrane area, and pressure, leads to a higher retentate temperature. Consequently, since the heat exchange within the reactor is limited, the conversion will be lower and to maintain an equivalent output, there will be a necessity to increase the input flow rate and to increase the volume of the reactor. (see Table 9)

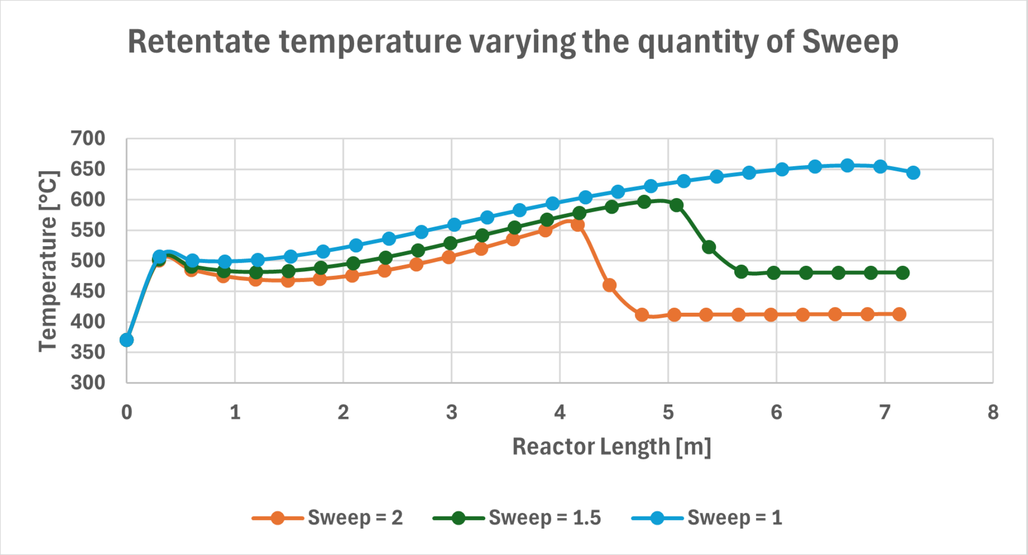

Figure 11: Temperature inside the membrane reactor by varying the Sweep gas

Table 9: Parameters of the membrane reactor varying the amount of sweep gas

Property	Sweep = 2	Sweep = 1.5	Sweep = 1	Unit
$T_{out_{RET}}$	412.55	480.56	644.49	$^{\circ}C$
N_2 Conversion	0.957	0.945	0.908	-
NH_3 Recovery	0.9994	0.9990	0.9945	-
V_{tot}	31.69	32.11	33.38	m^3
$InputMassFlowRate$	104.47	105.85	110.04	$\frac{ton}{day}$

Since the objective is to minimize the quantity of sweep gas to prevent over-sizing of plant components it has been chosen the minimum amount of sweep gas ($Sweep = 1 \cdot F_{in_{ret}}$). $F_{in_{ret}}$ is the total amount of feed entering in the retentate. Varying the inlet temperature of the sweep gas flowing into the permeate enables achieving higher conversion rates with reduced volume (refer to Fig. 12 and Table 10). Additionally, it allows to exploit the hydrogen produced from the PEM electrolyzer, which has a temperature of 80°C. Adopting this temperature eliminates the necessity for a heat exchanger, and given the hydrogen's pressure of 30 bar, eliminates the need for a compressor as well.

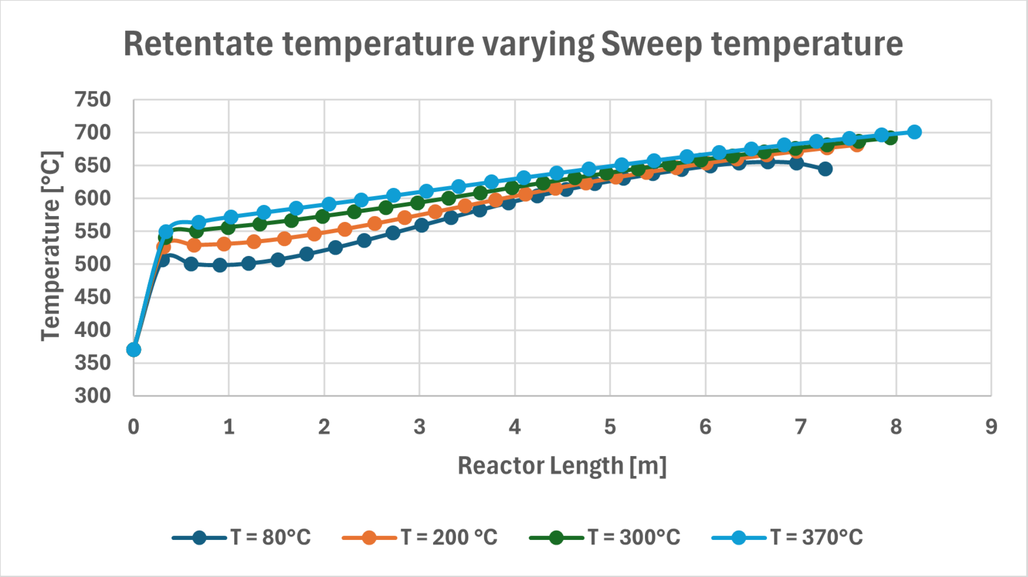

Figure 12: Temperature inside the membrane reactor by varying the Inlet temperature of the Sweep gas

Table 10: Parameters of the membrane reactor varying the temperature of sweep gas

Property	T = 370 °C	T = 300 °C	T = 200 °C	T = 80 °C	Unit
$T_{out_{RET}}$	701.15	691.92	681.59	644.69	$^{\circ}C$
N_2 Conversion	0.633	0.695	0.795	0.908	-
NH_3 Recovery	0.915	0.937	0.967	0.994	-
V_{tot}	47.94	43.68	38.16	33.38	m^3
$InputMassFlowRate$	158.04	143.83	125.8	110.04	$\frac{ton}{day}$

2.5.2 Effect of the Membrane Area

In table 11 are shown the data adopted for this set of simulation.

Table 11: Parameters of the membrane reactor

Property	Value	Unit
Inlet Temperature Ret	370	$^{\circ}C$
Inlet Temperature Ret	80	$^{\circ}C$
Inlet Retentate Pressure	200	bar
Inlet Permeate Pressure	30	bar
Sweep Gas	$1 \cdot Fin_{ret}$	$\frac{kmol}{hr}$
L/D ratio	3	$[-]$

In Figure 13, it can be observed that increasing the membrane area inside the reactor leads to a conversion plateau of approximately 0.91 at low space velocities. As shown in Figure 14, the ammonia recovery reaches its maximum for high membrane area values and low space velocity, indicating that all ammonia produced in the retentate manages to diffuse into the permeate, and the reaction is not limited by thermodynamics.

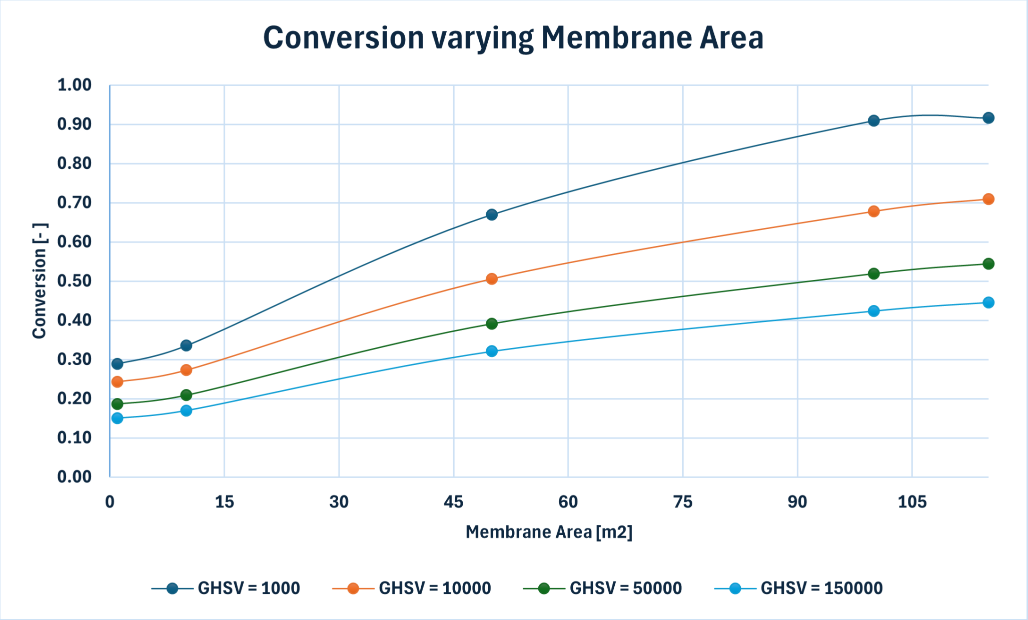

Figure 13: Conversion by varying the membrane area at different GHSV

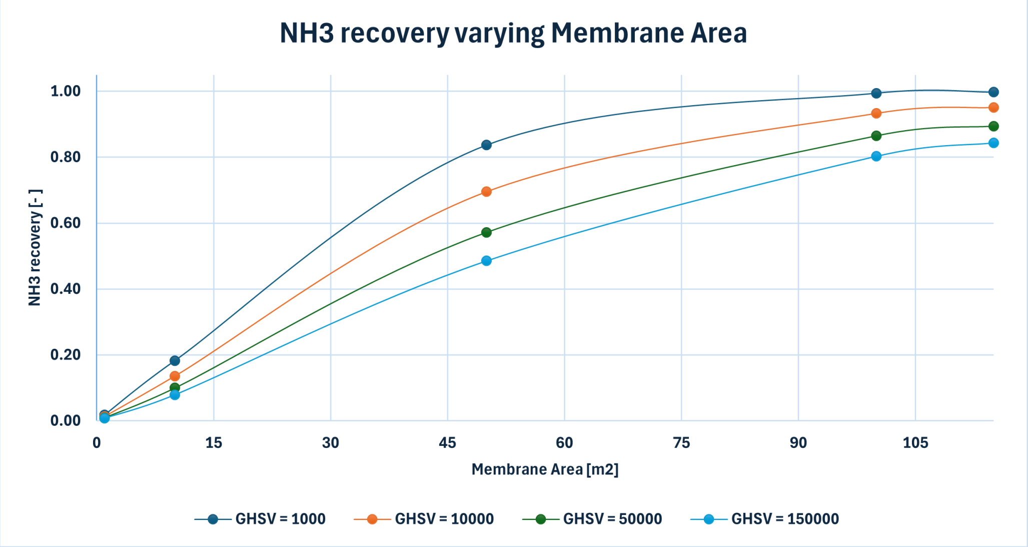

Figure 14: NH3 recovery by varying the membrane area at different GHSV

It is interesting to note how the temperatures at the exit of the retentate and permeate vary, as can be seen in Figure 15 and Figure 16. With the increase in membrane area, the temperature difference between the retentate and permeate decreases when both conversion and permeation are at their maximum. As illustrated in Fig. 17 plotting the temperature of the retentate, permeate, and conversion along the length of the reactor reveals that the reaction stops at a certain point, allowing the retentate to reach the temperature of the permeate. This is even more evident when comparing the case with Am = 115 (Fig. 18) to that with Am = 100 (Fig 17). The latter does not allow the reaction to stop, resulting in the retentate's exit temperature being much farther from that of the permeate.

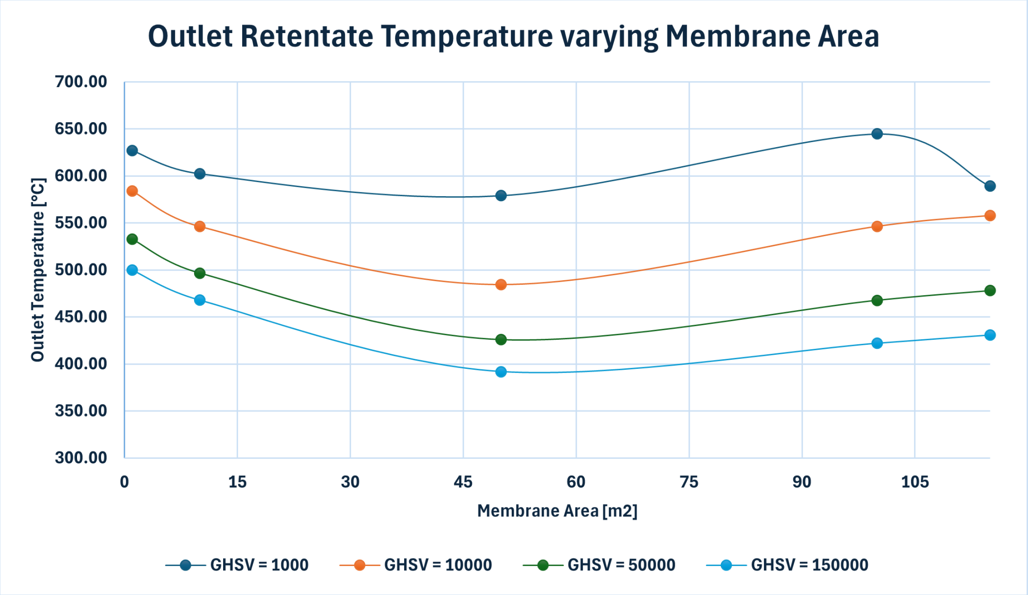

Figure 15: Outlet Temperature of the retentate

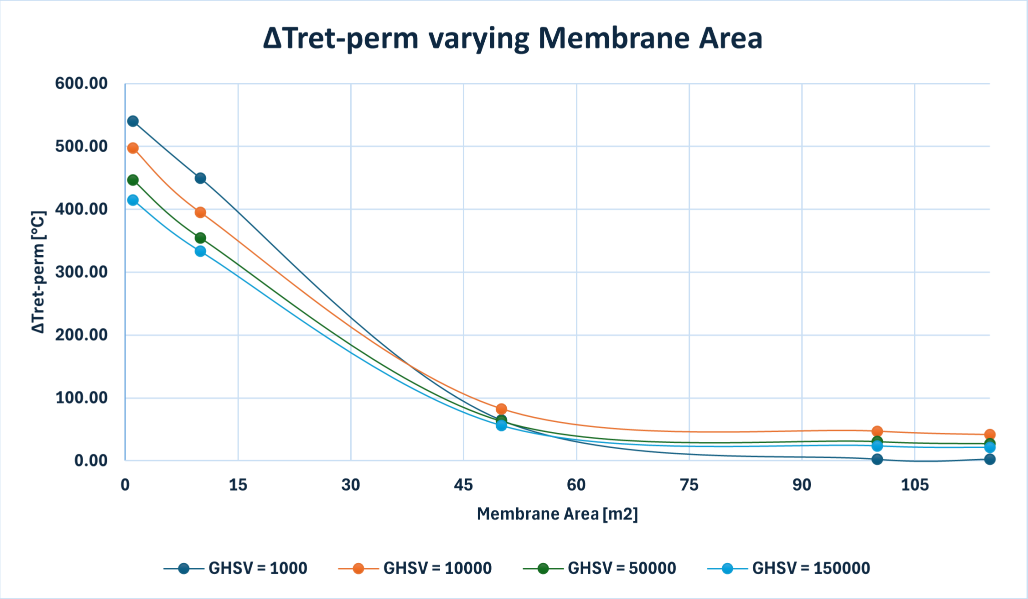

Figure 16: ΔT between Retentate and Permeate

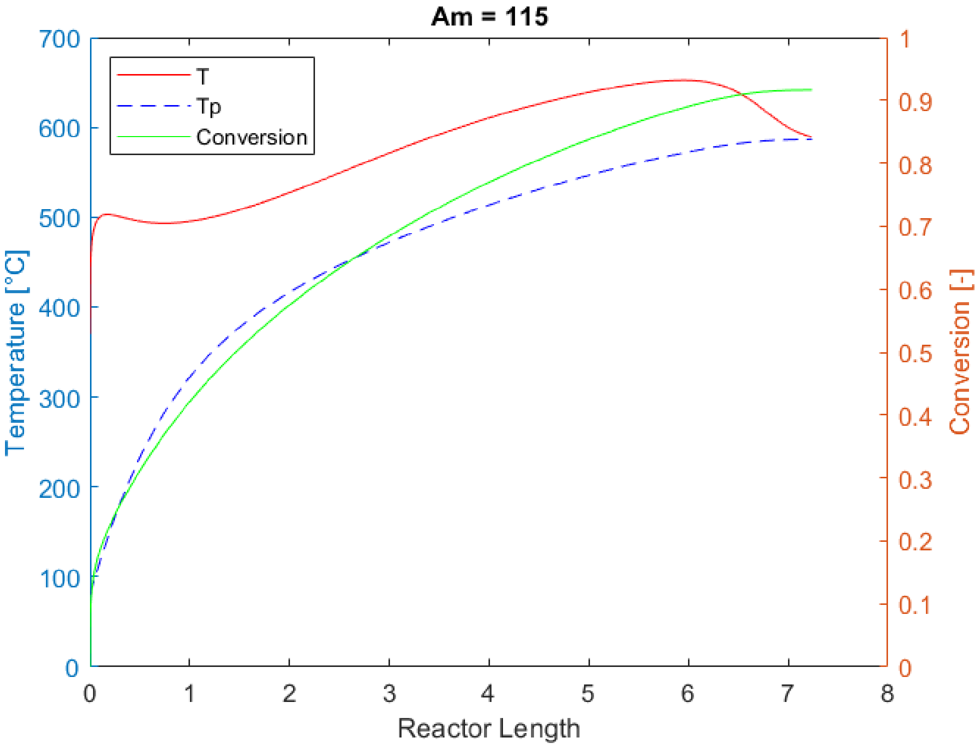

Figure 17: GHSV = 1000; Membrane area = 115 m^2

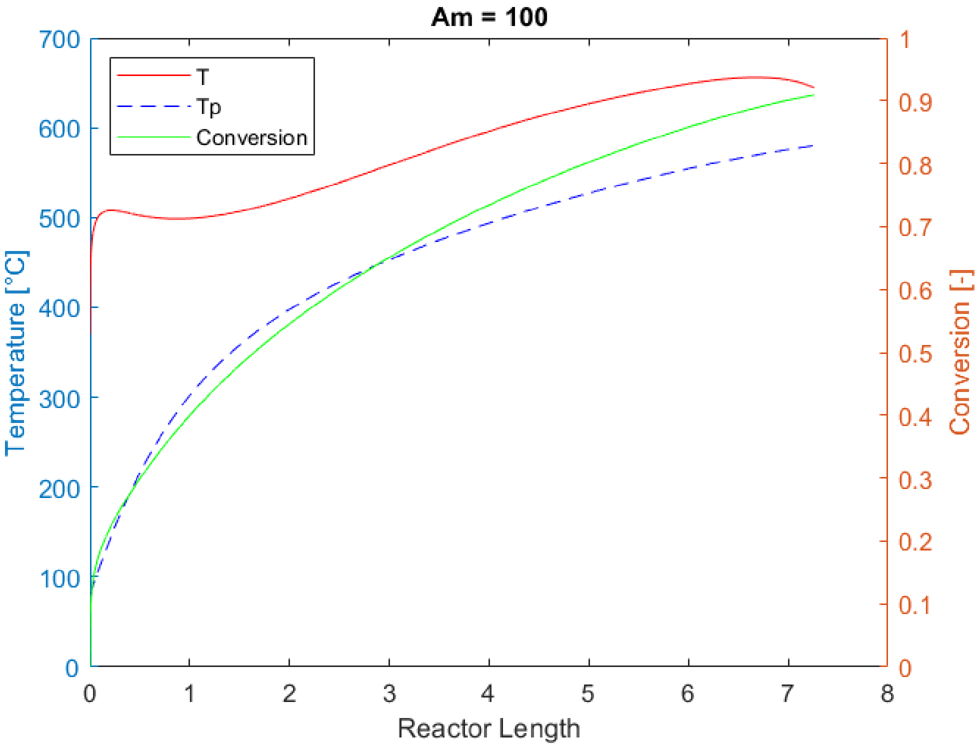

Figure 18: GHSV = 1000; Membrane area = 100 m^2

In the very initial moments when the feed is introduced into the reactor, a significant leap in conversion can be observed from the two figure above. This implies that the reaction rate is very high. After this jump, the conversion trend is monotonically increasing, which can be linked to the effect of the membrane capable of removing the produced ammonia, thus reducing its partial pressure in the retentate and favoring the formation of more ammonia.

3. Results

The assumptions made in this analysis are the same as those presented in the Aspen Model section.

For the conventional plant, an inlet temperature of 370°C is selected for each reactor based on Figure 9, which maximizes conversion. The unreacted gas from the flash, which separates the ammonia at a low temperature of -85°C, facilitates the cooling of the hot stream exiting the reactor. However, there's a necessity to utilize a refrigerant for the flow rate entering the second reactor. In Table 12 and Figure 19, it can observed the conversion rates, the temperatures, and the molar fraction of each species exiting each reactor. To maintain the same GHSV, considering that the reaction leads to a decrease in moles, the volumes of the second and third reactors will progressively decrease. Furthermore, the conversion rate will also decrease due to the formation of ammonia. The overall conversion with respect of the N_2 entering the first reactor and the N_2 exiting the third one is equal to 53%. The thermodynamic points of the cycle are shown in Table 13.

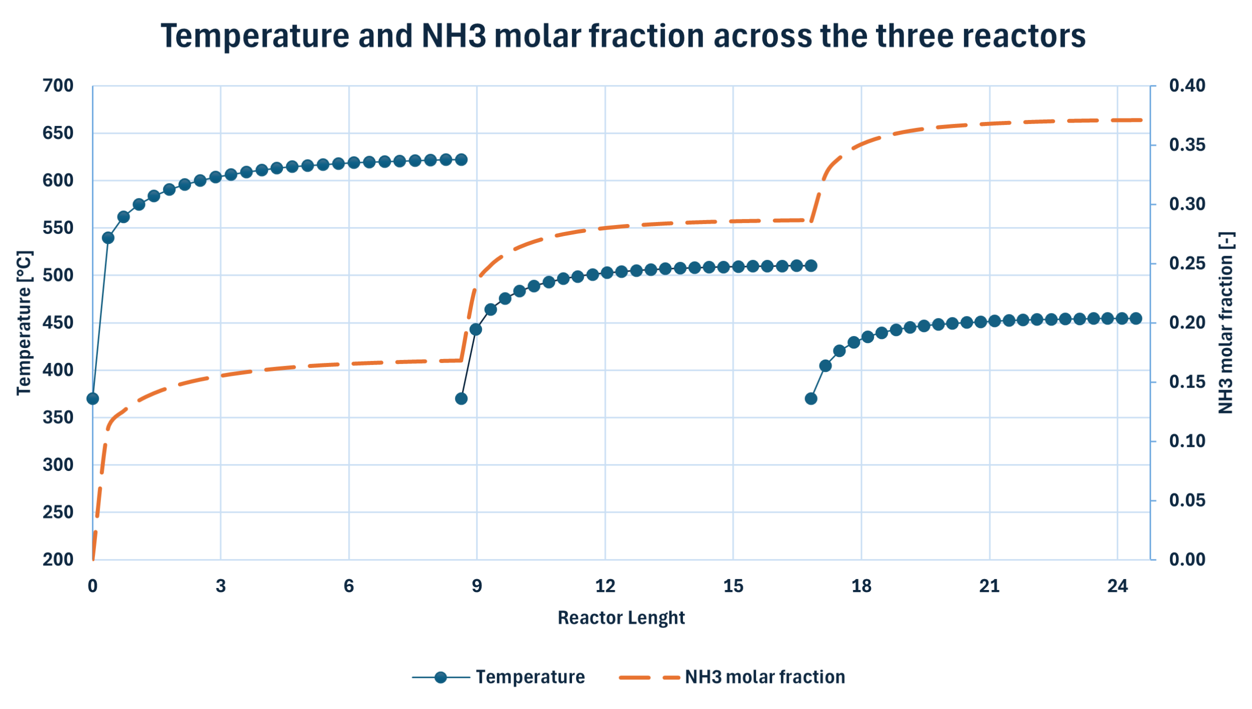

Figure 19: NH_3 molar fraction and temperature of the feed across the reactors

Table 12: Parameters at the exit of each reactor in the conventional process

Parameter	First reactor	Second Reactor	Third Reactor	Unit
N_2 Conversion	0.29	0.22	0.17	-
T_{in}	370	370	370	°C
T_{out}	622	510	455	°C
y_{H2}	0.62	0.54	0.17	-
y_{N2}	0.21	0.18	0.16	-
y_{NH3}	0.17	0.29	0.37	-
$Length$	8.63	8.19	7.93	m
$Diamter$	2.88	2.73	2.64	m
$Volume$	56.09	48.01	43.58	m^3
Catalyst weight	31.41	26.89	24.41	ton

Table 13: Thermodynamic points of the cycle with the conventional reactors

Stream	Temperature [°C]	Pressure [bar]	Mass Flow [ton/day]	N2 [-]	H2 [-]	NH3 [-]
FEED	80.00	30	100.11	0.25	0.75	0
FEEDHP	370.18	200	100.11	0.2500	0.7500	0
INPUT	370.00	200	184.97	0.2499	0.7498	0.003
INPUT2	370.00	200	184.97	0.2079	0.6237	0.1684
INPUT3	370.00	200	184.97	0.1783	0.5348	0.2870
INSEP	-85.00	200	184.97	0.1571	0.4711	0.3718
NH3	-85.00	200	100.11	0.0000	0.0002	0.9998
OUT1	622.00	200	184.97	0.2079	0.6237	0.1684
OUT11	544.00	200	184.97	0.2079	0.6237	0.1684
OUT2	510.32	200	184.97	0.1783	0.5348	0.2870
OUT3	454.76	200	184.97	0.1571	0.4711	0.3718
REC1	-85.00	200	84.86	0.2499	0.7495	0.006
REC2	194.933	200	84.86	0.2499	0.7495	0.006
REC3	369.974	200	84.86	0.2499	0.7495	0.006

For the plant utilizing the membrane reactor, various parameters influence both the conversion and the dimensions of the membrane reactor, as previously observed. Table 14 presents the parameters characterizing the reactor, while Figures 21 and 22 illustrate the trends of partial pressures in the retentate and permeate, respectively. Additionally, Figure 20 depicts the temperature and conversion trends along the axial coordinate of the reactor. Examining these figures, it can be observed that hydrogen is the limiting reagent, reaching a much lower partial pressure compared to nitrogen in the retentate. Ammonia reaches a peak concentration and then, due to the membrane effect, is linearly separated until the reaction ceases, achieving optimal separation. In contrast, within the permeate, there is a continuous increase of ammonia followed by a steady decrease of reactants, until maximum conversion is achieved.The thermodynamic points of the cycle are shown in Table 15.

Table 14: Membrane reactor parameters

Parameter	Value	Unit
$T_{in_{RET}}$	370	$^{\circ}C$
$T_{in_{PERM}}$	80	$^{\circ}C$
$T_{out_{RET}}$	589	$^{\circ}C$
$T_{out_{PERM}}$	586	$^{\circ}C$
$P_{in_{RET}}$	200	bar
$P_{in_{PERM}}$	30	bar
$Sweep_{gas}$	$F_{in_{ret}}$	$\frac{kmol}{hr}$
A_m	115	m^2
N_m	505	$-$
L	7.245	m
D	2.415	m
V_{tot}	33.192	m^3
NH_3 Recovery	0.9975	-
Catalyst weight	18.587	ton
$GHSV$	1000	$\frac{1}{h}$
$Mass_{flowrate}$	109.84	$\frac{ton}{d}$
$NH_3 output$	100	$\frac{ton}{day}$

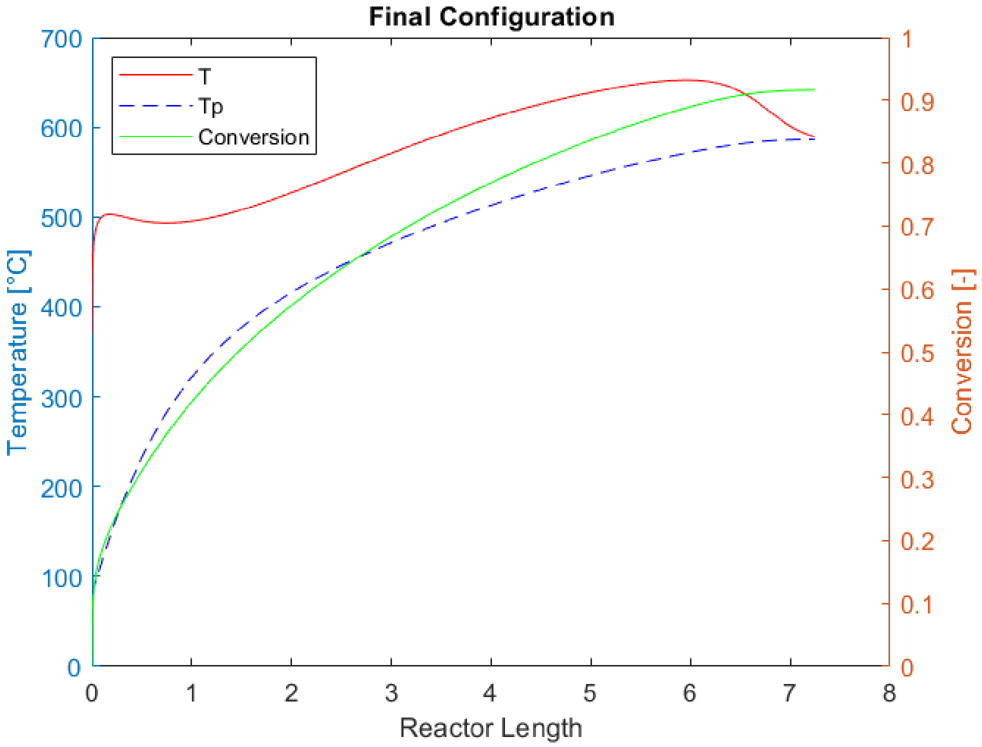

Figure 20: Temperature and Conversion inside the reactor

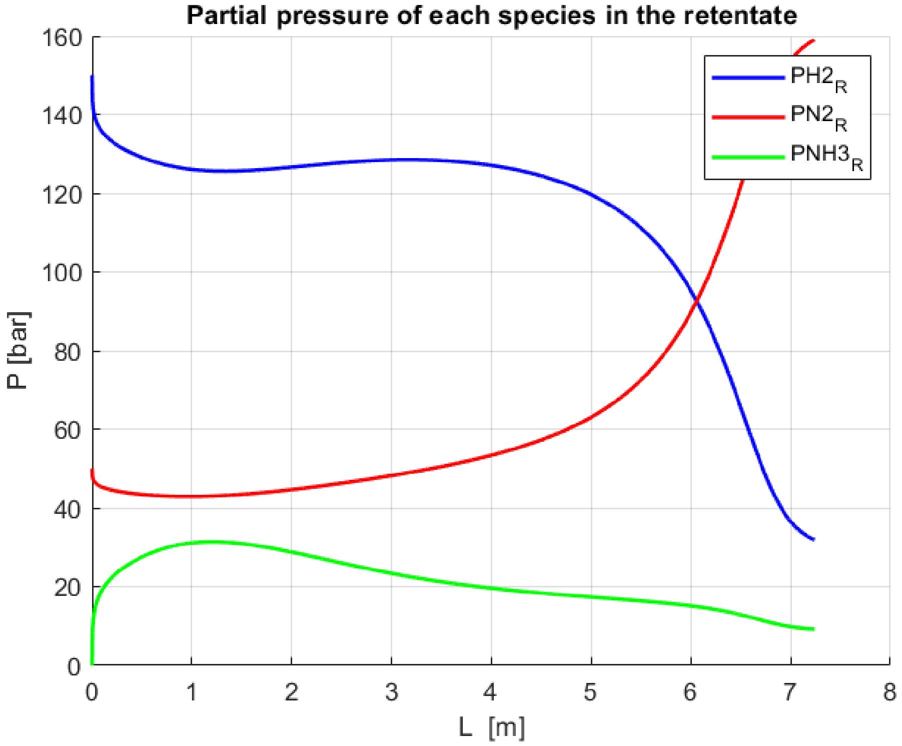

Figure 21: Partial pressure of each species in the retentate

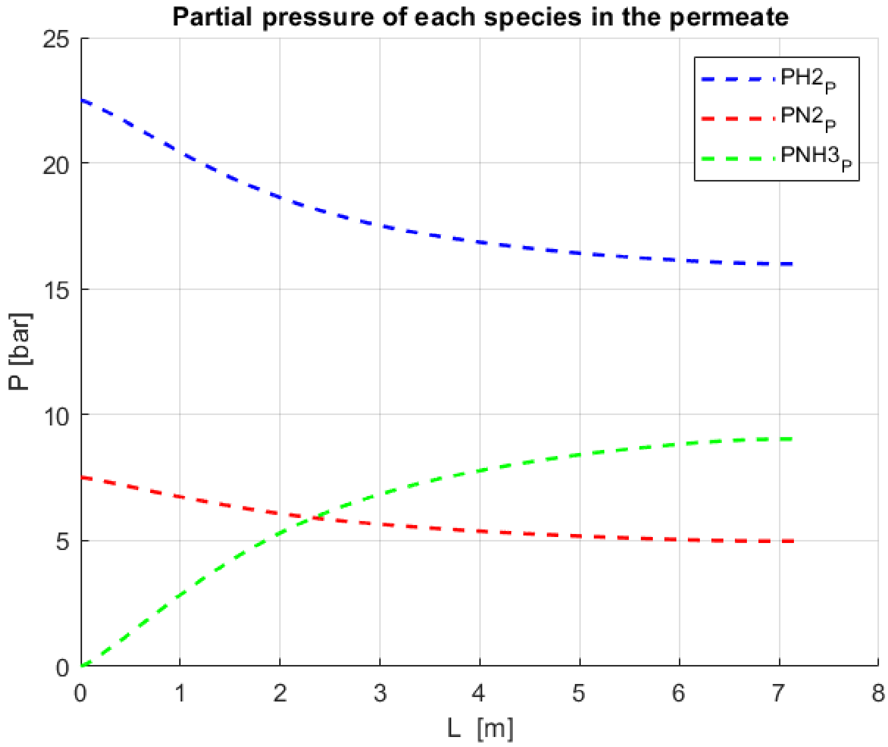

Figure 22: Partial pressure of each species in the permeate

Table 15: Thermodynamic points of the cycle with the conventional reactors

Stream	Temperature [°C]	Pressure [bar]	Mass Flow [ton/day]	N2 [-]	H2 [-]	NH3 [-]
FEED	80	30	100.11	0.2500	0.7500	0
FEEDHP	370.18	200	100.11	0.2500	0.7500	0
INPUTR	370	200	109.84	0.2497	0.7492	0.0011
INPUTP	80	30	109.84	0.2499	0.7497	0.0005
INSEP	-85	30	209.95	0.1716	0.5148	0.3136
NH3	-85	200	100.11	0.0000	0.0002	0.9998
OUTP	586.42	30	209.95	0.1716	0.5148	0.3136
OUTPC	496.75	30	209.95	0.1716	0.5148	0.3136
OUTR	589.44	200	9.73	0.2468	0.7402	0.0130
RECP	-85	30	109.95	0.2499	0.7497	0.0005

Table 16 presents the dimensions of each component in the two different plants. The plant with conventional reactors in a closed loop has a lower conversion rate and requires larger heat exchangers due to the higher heat duty, as compared to the plant using a membrane reactor. This difference is further illustrated in Table 17. The refrigerant fluid flow rate and the exchanged power are higher in the membrane system compared to the conventional system due to a 10% increase in flow rate. Specifically, Ethane is used as the refrigerant, with the membrane system utilizing 1050 tons/day in the closed refrigeration cycle, compared to 905 tons/day in the conventional system.

Table 16: Components size

Equipment	Conventional plant	Membrane plant	Unit
COMP	1284.08	1284.08	kW
HX1	2.252	1.435	m^2
HX2	6.334	-	m^2
HX3	3.074	-	m^2
Cooler	79.3242	86.5727	m^2
Separator	3.3	3.3	ton
Reactor	147.7	33.19	m^3

Table 17: Heat Exchanger Heat Duty

Equipment	Conventional plant	Membrane plant	Unit
HX1	578	716	kW
HX2	-1262	-	kW
HX3	995	-	kW
Cooler	-5071	-5920	kW

In Figure 23, it can be observed that the cost of reactors in the conventional plant is significantly higher than that of the membrane plant. This is attributed to lower conversion and larger volumes required. Additionally, Figure 24 and 25 indicate that the compressor is the most expensive component in both plants, followed by the cooler, which, using ethane as a refrigerant, allows the temperature to reach -85°C before separation occurs. The main difference in cost distribution is due to the series of three reactors in the conventional plant shown in Figure 22, which have a total volume 4.4 times greater than the single membrane reactor. Table 16 shows that the difference in Total Overnight Costs is nearly 3.7 million euros.

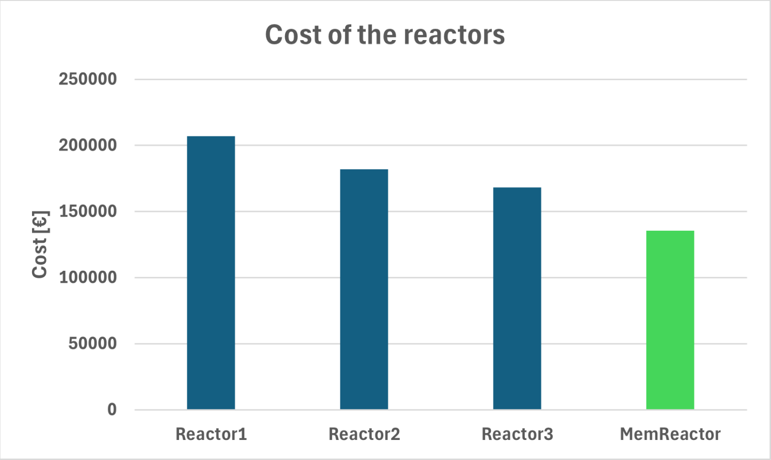

Figure 23: Comparison of reactor's costs

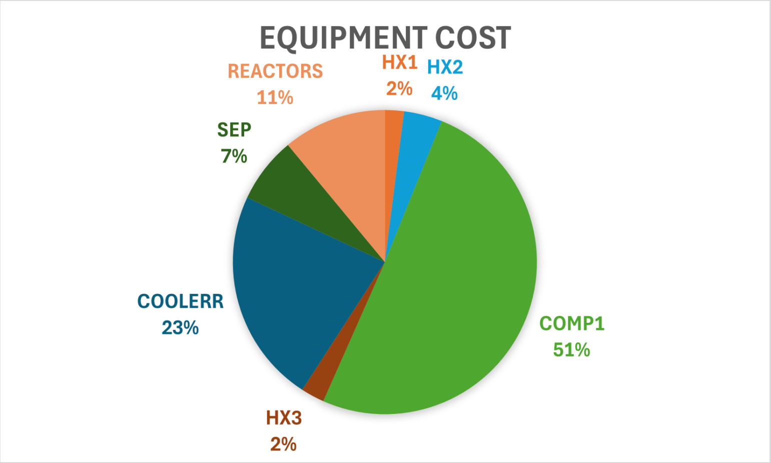

Figure 24: Equipment costs of the conventional plant

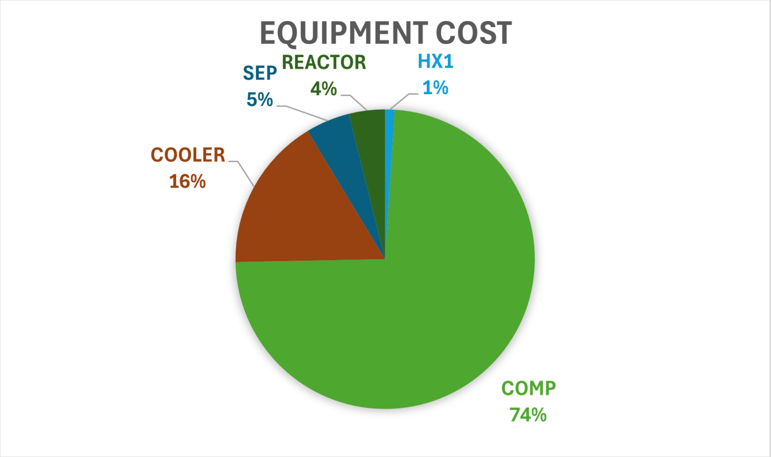

Figure 25: Equipment costs of the membrane plant

Table 18: Costs related to CAPEX

Parameter	Conventional plant	Membrane plant	Unit
BEC	5.06	3.46	M€
TIC	4.04	2.77	M€
TDPC	9.10	6.23	M€
IC	1.27	0.87	M€
EPC	10.37	7.11	M€
Contingecy	1.03	0.71	M€
Owner's cost	0.52	0.35	M€
C&OC	1.55	1.06	M€
TOC	**11.94**	**8.17**	M€

Regarding OPEX, they have the greatest impact on the final cost of ammonia. Feed-related costs are identical since both plants achieve the same final conversion due to recirculation. The only differences lie in utility and fixed costs. Utility costs include the total electricity used mainly by the compressor and the electricity and refrigerant used in the refrigeration cycle for both plants. Additionally, for the conventional plant, utility costs also encompass the electricity and cooling water used in the second heat exchanger. For the membrane reactor, utility costs also include the costs of sweep gas. The total electricity used is **1380.2 kWh** for the conventional plant and **1336.4 kWh** for the membrane plant. The difference in fixed OPEX is attributed to the Total Operating Cost (TOC), which is higher in the conventional plant. Table Y summarizes the three components that contribute to the calculation of total OPEX.

Table 19: Summary of the OPEX

Parameter	Conventional plant	Membrane plant	Unit
Utilities	0.948	0.912	M€
Feedstock	34.479	34.479	M€
Fixed	0.658	0.424	M€
Total	**36.086**	**35.816**	M€

The main KPI of this analysis is the cost of ammonia production, which is lower for the membrane plant compared to the conventional one

Table 20: Cost of Ammonia produced

Parameter	Conventional plant	Membrane plant	Unit
COP_{NH_3}	**1136**	**1117**	$\frac{€}{ton}$

The same analysis was also conducted using an operating pressure of 100 bar, and the difference between the two prices of produced ammonia further reduces to 8 euros per ton, demonstrating that what matters most is the quantity of reagents to be introduced rather than the components used within the plant. Comparing these results with those from other studies reveals that these values fall within the expected ranges when PEM electrolyzers are used, but they are significantly different from those produced by conventional hydrogen production methods, such as steam reforming. However, these comparisons are limited by the differing approaches and hypotheses employed.

4. Conclusions and future developments

The main goal of this techno-economic analysis was the design and optimization of the membrane catalytic reactor for ammonia synthesis, to replace the reactors used in the conventional plant. These two types of reactors were initially studied and designed in MATLAB. Subsequently, to determine the optimal configuration, they were implemented in Aspen PLUS for a techno-economic analysis, which highlighted that the plant equipped with a membrane reactor is slightly better because it results in a slightly lower cost of ammonia.

Focusing on single-pass conversion, the membrane reactor configuration proves highly advantageous compared to the conventional one. It allows for a single reactor and smaller volumes to achieve the same output. This advantage isn't evident when recirculation is employed within the Haber process. The potential benefit of employing a membrane reactor over a series of reactors lies in utilizing fewer components within the plant.

Unlike the conventional Haber-Bosch process, it was assumed that hydrogen is produced from an electrolyzer and nitrogen from a PSA (Pressure Swing Adsorption) system. This approach aims to reduce CO2 emissions associated with this highly energy-intensive process.

What most influences the price of produced ammonia is the cost of hydrogen. The advantage of membrane reactors is that they require fewer components within the plant. This combined effect, along with new research on catalysts that can lower process temperatures and operating pressures, and especially enable non-stoichiometric hydrogen-nitrogen ratios in the reaction, could lead to a significant reduction in the cost of produced ammonia. It should be noted that conventional ammonia separation methods were used in this study because the focus was on the design and optimization of the membrane reactor. However, new methods of ammonia separation can certainly impact the final price of ammonia.

5. Bibliography

References

[1] Shahmir Ali Nosherwani and Rui Costa Neto. Techno-economic assessment of commercial ammonia synthesis methods in coastal areas of Germany. *Journal of Energy Storage*, 34:102201, February 2021.

[2] Richard Nayak-Luke, René Bañares-Alcántara, and Ian Wilkinson. "Green" Ammonia: Impact of Renewable Energy Intermittency on Plant Sizing and Levelized Cost of Ammonia. *Industrial & Engineering Chemistry Research*, 57(43):14607–14616, October 2018.

[3] Limitations of Ammonia as a Hydrogen Energy Carrier for the Transportation Sector | ACS Energy Letters.

[4] Oscar Serpell. Ammonia's Role in a Net-zero Hydrogen Economy.

[5] The Royal Society. Ammonia: zero-carbon fertiliser, fuel and energy store.

[6] Collin Smith, Alfred K. Hill, and Laura Torrente-Murciano. Current and future role of Haber–Bosch ammonia in a carbon-free energy landscape. *Energy & Environmental Science*, 13(2):331–344, 2020.

[7] Introduction to Membrane.

[8] John L Falconer, Richard D Noble, and David P Sperry. Catalytic membrane reactors.

[9] John Humphreys, Rong Lan, and Shanwen Tao. Development and Recent Progress on Ammonia Synthesis Catalysts for Haber–Bosch Process. *Advanced Energy and Sustainability Research*, 2(1):2000043, January 2021.

[10] Jayant M Modak. Haber Process for Ammonia Synthesis. 2011.

[11] J.A. Medrano, M.A. Llosa-Tanco, D.A. Pacheco-Tanaka, and F. Gallucci. Transport Mechanism and Modeling of Microporous Carbon Membranes. In *Current Trends and Future Developments on (Bio-) Membranes*, pages 39–58. Elsevier, 2019.

[12] Hannes Richter, Hartwig Voss, Nadine Kaltenborn, Susanne Kämnitz, Alexander Wollbrink, Armin Feldhoff, Jürgen Caro, Stefan Roitsch, and Ingolf Voigt. High-Flux Carbon Molecular Sieve Membranes for Gas Separation. *Angewandte Chemie International Edition*, 56(27):7760–7763, 2017. _eprint: https://onlinelibrary.wiley.com/doi/pdf/10.1002/anie.201701851.

[13] Masakoto Kanezashi, Akira Yamamoto, Tomohisa Yoshioka, and Toshinori Tsuru. Characteristics of ammonia permeation through porous silica membranes. *AIChE Journal*, 56(5):1204–1212, 2010. _eprint: https://onlinelibrary.wiley.com/doi/pdf/10.1002/aic.12059.

[14] D. C. Dyson and J. M. Simon. Kinetic Expression with Diffusion Correction for Ammonia Synthesis on Industrial Catalyst. *Industrial & Engineering Chemistry Fundamentals*, 7(4):605–610, November 1968.

[15] Ilenia Rossetti, Nicola Pernicone, Francesco Ferrero, and Lucio Forni. Kinetic Study of Ammonia Synthesis on a Promoted Ru/C Catalyst. *Industrial & Engineering Chemistry Research*, 45(12):4150–4155, June 2006. Publisher: American Chemical Society.

[16] Anders Nielsen, Jørgen Kjaer, and Bennie Hansen. Rate equation and mechanism of ammonia synthesis at industrial conditions. *Journal of Catalysis*, 3(1):68–79, February 1964.

[17] Shriniwas S. Chauk and Liang-Shih Fan. HEAT TRANSFER IN PACKED AND FLUIDIZED BEDS. In Warren M. Rohsenow, James P. Hartnett, and Young I. Cho, editors, *Handbook of Heat Transfer*. McGraw-Hill Education, 1st edition edition, 1998.

[18] J. Dirker and Josua Meyer. Convective Heat Transfer Coefficients in Concentric Annuli. *Heat Transfer Engineering - HEAT TRANSFER ENG*, 26:38–44, March 2005.

[19] Serena Poto, Fausto Gallucci, and M. Fernanda Neira d'Angelo. Direct conversion of CO2 to dimethyl ether in a fixed bed membrane reactor: Influence of membrane properties and process conditions. *Fuel*, 302:121080, October 2021.

[20] Kristin Gerdes, William Summers, and John Wimer. Quality Guidelines for Energy System Studies: Cost Estimation Methodology for NETL Assessments of Power Plant Performance. Technical Report DOE/NETL-2011/1455, 1513278, August 2011.

[21] Richard Turton, Richard C. Bailie, Wallace B. Whiting, Joseph A. Shaeiwitz, and Debangsu Bhattacharyya. *Analysis, synthesis, and design of chemical processes*. Prentice Hall international series in the physical and chemical engineering sciences. Prentice Hall, Upper Saddle River, N.J. Munich, fourth edition edition, 2012.

[22] G. Manzolini, E. Sanchez Fernandez, S. Rezvani, E. Macchi, E.L.V. Goetheer, and T.J.H. Vlugt. Economic assessment of novel amine based CO2 capture technologies integrated in power plants based on European Benchmarking Task Force methodology. *Applied Energy*, 138:546–558, January 2015.

[23] Yaroslav Grosu, Abdessamad Faik, Iñigo Ortega-Fernández, and Bruno D'Aguanno. Natural Magnetite for thermal energy storage: Excellent thermophysical properties, reversible latent heat transition and controlled thermal conductivity. *Solar Energy Materials and Solar Cells*, 161:170–176, March 2017.

[24] Danlin Chen, Feng Yang, Dionysis S. Karousos, Linfeng Lei, Evangelos P. Favvas, and Xuezhong He. Process parametric testing and simulation of carbon membranes for H2 recovery from natural gas pipeline networks. *Separation and Purification Technology*, 307:122842, February 2023.

[25] Carlos Arnaiz Del Pozo and Schalk Cloete. Techno-economic assessment of blue and green ammonia as energy carriers in a low-carbon future. *Energy Conversion and Management*, 255:115312, March 2022.

Abstract in lingua italiana

L'ammoniaca giocherà un ruolo cruciale nei prossimi anni per aiutare l'Europa a raggiungere i suoi obiettivi energetici. Può essere utilizzata come vettore di idrogeno grazie alle sue proprietà superiori: può essere liquefatta a temperature e pressioni molto più gestibili, ha una migliore densità energetica volumetrica e non è infiammabile. Questi vantaggi, insieme alla solida infrastruttura pre-esistente dell'ammoniaca, potrebbero risolvere i problemi di stoccaggio e trasporto associati all'idrogeno.
Questo studio prevede un'analisi tecnico-economica di un impianto che utilizza un reattore catalitico a membrana per la sintesi dell'ammoniaca, confrontato con uno che impiega reattori convenzionali. L'obiettivo di produzione è di 100 tonnellate di ammoniaca al giorno. Il reattore a membrana si dimostra molto più efficiente rispetto alla serie di reattori tradizionali, in quanto raggiunge il target con tassi di conversione più elevati e volumi e quantità di catalizzatori minori. A differenza della serie di tre reattori convenzionali, il reattore a membrana non richiede raffreddamento per aumentare la conversione e superare i limiti termodinamici della reazione.
L'analisi tecnico-economica dimostra che l'impianto dotato di reattore a membrana è leggermente migliore rispetto a quello convenzionale. Il reattore a membrana consente di utilizzare meno componenti all'interno dell'impianto. Il costo principale è legato al feed in ingresso, che rimane lo stesso in entrambi i casi a causa del riciclo dei reagenti non convertiti nel processo Haber-Bosch.

Parole chiave: Aspen Plus, Analisi tecnico-economica, Haber-Bosch, Idrogeno, MATLAB, Reattore catalitico a membrana, Sintesi dell'ammoniaca in italiano

Acknowledgements